1998-10-01

Reactions of Chlorine Atoms with Aromatic Compounds

Barbara O'Leary
Dublin Institute of Technology

REACTIONS OF CHLORINE ATOMS WITH AROMATIC COMPOUNDS

A thesis submitted to

DUBLIN INSTITUTE OF TECHNOLOGY

for the degree of

MASTER OF PHILOSOPHY

by

BARBARA O'LEARY B.Sc. (Hons.)

Based on research carried out in

School of Chemistry, Dublin Institute of Technology, Kevin St.

and

Laboratoire de Combustion et Systèmes Réactifs, Centre Nationale de la Recherche Scientifique, Orléans, France

under the supervision of

Dr. Jack Treacy

Dublin Institute of Technology, Kevin St. October 1998

Declaration

I certify that this thesis which I now submit for examination for the award of Master of Philosophy, is entirely my own work and has not been taken from the work of others save and to the extent that such work has been cited and acknowledged within the text of my work.

This thesis was prepared according to the regulations for postgraduate studies by research of the Dublin Institute of Technology and has not been submitted in whole or in part for an award in any other Institute or University.

The Institute has pemission to keep, to lend or to copy this thesis in whole or part, on condition that any such use of the material of the thesis be duly acknowledged.

Signature Barbara O'Leary Date 05/99

Acknowledgements

I would like to express my deepest gratitude to my supervisor Dr. Jack Treacy for all his help and guidance during the research and preparation of this thesis. Many thanks also to Dr. Howard Sidebottom of U.C.D. for his advice and interest in this work.

Warmest thanks go to my colleagues in the lab, Mary, John and Paul. Their friendship has been much appreciated as well as their unfailing eagerness to discuss atmospheric problems in more comfortable surroundings! Thanks also to all the other chemistry postgraduates and technicians in Kevin St. for their friendship and many good nights out.

I would like to thank all the people in the atmospheric chemistry section in Orléans, particularly Alberto, Wahid and Régis, who made my visit so fruitful and enjoyable. Thanks are due to all the atmospheric chemists in UCD for their help and friendship.

To all my non-chemistry friends, I extend my thanks for their friendship and support during my post-graduate years and for pretending to find atmospheric chemistry interesting.

Finally I would like to thank my family for their encouragement throughout my student years. My parents have never faltered in supporting me, both financially and emotionally, and for this I am immensely grateful.

Contents

Figure Captions

Table Captions

Abstract

This thesis presents the results of kinetic studies on the reactions of chlorine atoms with a series of aromatic compounds. The rate constants (in units of 10^{-11} cm^3 molecule^{-1} s^{-1}) for the following reactions were determined at 298 ± 2 K using a relative rate technique: (Cl + benzene < 0.1), (Cl + toluene = 6.70 ± 0.41), (Cl + toluene-$\mathbf{d_8}$ = 3.75 ± 0.24), (Cl + *o*-xylene = 16.9 ± 0.8), (Cl + *o*-xylene-$\mathbf{d_{10}}$ = 13.7 ± 1.0), (Cl + *m*-xylene = 15.0 ± 0.8), (Cl + *p*-xylene = 19.1 ± 0.6), (Cl + *p*-xylene-$\mathbf{d_{10}}$ = 10.1 ± 0.6), (Cl + *p*-xylene-$\mathbf{d_6}$ = 10.4 ± 0.6), (Cl + 1,3,5-trimethylbenzene = 26.8 ± 1.8), (Cl + 1,2,4,5-tetramethylbenzene = 28.8 ± 1.5), (Cl + *o*-ethyltoluene = 21.9 ± 1.0), (Cl + *m*-ethyltoluene = 22.1 ± 1.1), Cl + *p*-ethyltoluene = 20.7 ± 0.8), (Cl + ethylbenzene = 12.3 ± 0.3), (Cl + n-propylbenzene = 21.9 ± 0.6), (Cl + n-butylbenyene = 28.0 ± 1.8), (Cl + 2-fluorotoluene = 3.38 ± 0.36), (Cl + 3-fluorotoluene = 3.34 ± 0.26), (Cl + 4-fluorotoluene = 4.96 ± 0.45), and (Cl + 2-chlorotoluene = 4.94 ± 0.79).

Room temperature rate constants (in units of 10^{-11} cm^3 molecule^{-1} s^{-1}) for the following reactions were also determined using the absolute technique of pulsed laser photolysis - resonance fluorescence:
(Cl + 2-fluorotoluene = 2.87 ± 0.16), (Cl + 3-fluorotoluene = 4.00 ± 0.15), and (Cl + 4-fluorotoluene = 5.67 ± 0.26).

The mechanism for these chlorination reactions was also investigated. The good correlation between log k_{Cl} and log k_{NO3} for a series of aromatics combined with the poor correlation between log k_{Cl} and log k_{OH} strongly suggests that the dominant pathway for reaction with chlorine atoms is H-atom abstraction from the alkyl substituent(s). The observed increase in reactivity with increasing length of the alkyl side chain is further support for this mechanism. Finally, the existence of a strong kinetic isotope effect between selected aromatics and their deuterated analogues provides additional evidence that the dominant if not exclusive reaction channel is H-atom abstraction.

In general the reactivity of chlorine atoms towards aromatic compounds is one to two orders of magnitude greater than that of hydroxyl radicals. Hence, should the ambient concentration of chlorine atoms be in the range 10^3 - 10^5 per cm^3, atmospheric loss through reaction with chlorine atoms will be significant and of the same order as that from reaction with hydroxyl radicals.

Chapter 1

General Introduction

1.1. STRUCTURE AND CHEMISTRY OF THE ATMOSPHERE

The earth is surrounded by a layer of gases approximately 500 km thick known as the atmosphere. The atmosphere is stratified on the basis of temperature. Fig. 1.1. shows the change in temperature and pressure with altitude; pressure decreases steadily with increasing distance from the surface of the earth whereas the variation in temperature is more erratic.

The temperature of the atmosphere decreases steadily from the surface of the earth until it reaches a minimum of 217 K at an altitude of 10-16 km. This minimum is known as the tropopause and the region of the atmosphere below this is the troposphere. Above the tropopause is a region called the stratosphere where the temperature increases to 271 K at the stratopause situated at 50 km above the earth's surface. Between 50 km and 85 km is the mesosphere where the temperature decreases to a minimum of 181 K at the mesopause. The outermost layer of the atmosphere is the thermosphere where the temperature reaches 1470 K. The region beyond the thermosphere is known as the exosphere.

1.1.1. The Ionosphere and the Exosphere

The mesosphere and thermosphere together are known as the ionosphere. Most of the sun's ionising radiation is absorbed in this region causing the ionisation of species present.

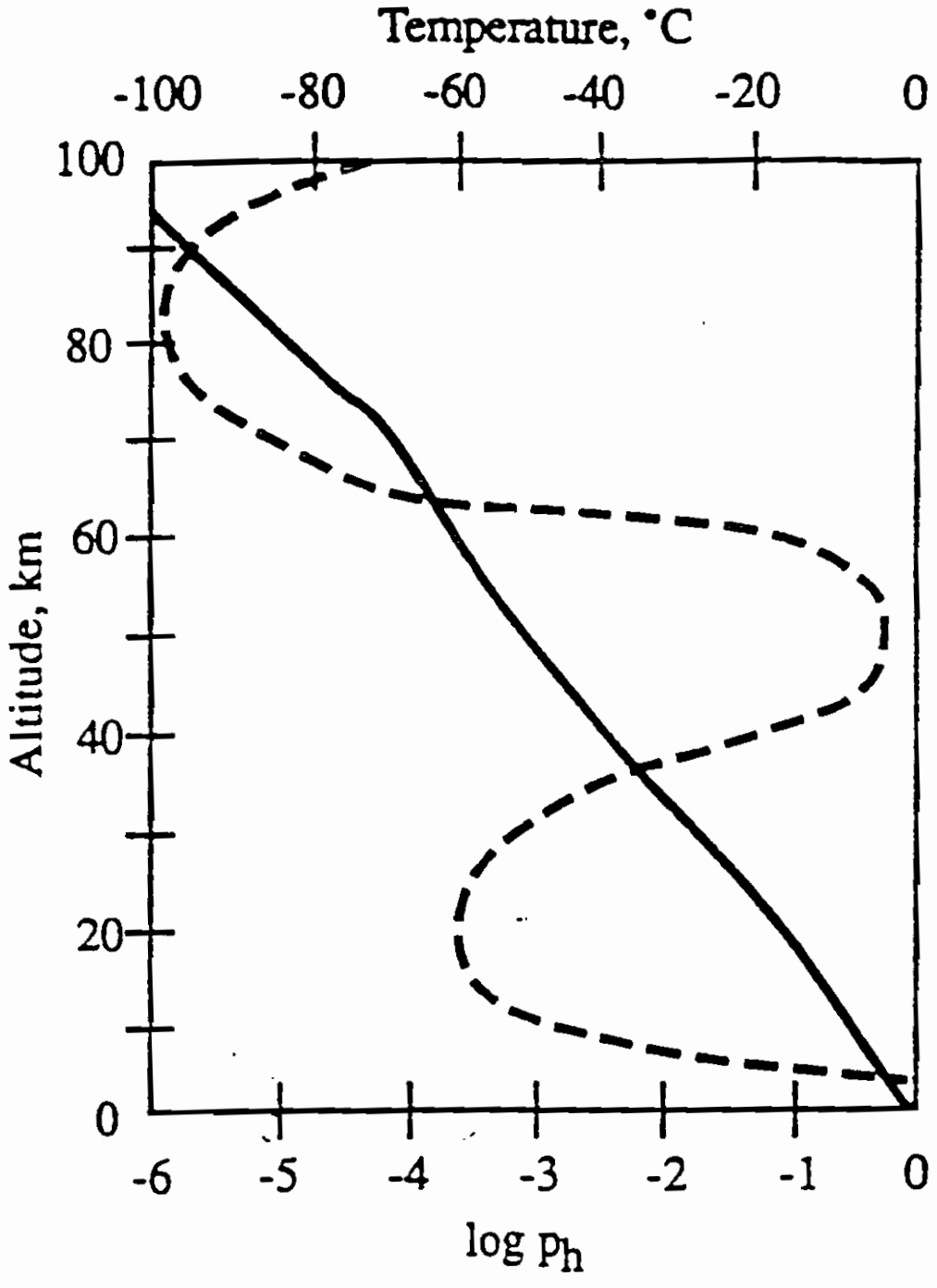

Figure 1.1. Structure of the atmosphere showing the variation of temperature and pressure with altitude.

The most abundant ions in the ionosphere are O_2^+, O^+ and NO^+. The phenonomen known as the Aurora, when displays of coloured lights are seen in the sky near the poles, occurs when streams of charged particles from the sun (the solar wind) ionize atmospheric gases. The exosphere merges with the interplanetary medium and has no definite outer boundary. It is very rarefied and consists of hydrogen and helium with some atoms of oxygen at lower altitudes (up to 600 km).

1.1.2. The Stratosphere

The chemistry of the stratosphere is dominated by ozone. Ozone is present throughout the troposphere, stratosphere and lower mesosphere but it reaches a peak in concentration in the lower stratosphere, at an altitude of 20-25 km. This is known as the ozone layer. Ozone is vital to life on earth as it protects plants and animals from the sun's harmful ultra-violet radiation via the following reaction:

$$O_3 + h\nu\ (\lambda = 220\text{-}315\ nm) \rightarrow O(^1D) + O_2 \qquad (1.1)$$

In 1930 Chapman [1] proposed a theory to explain the concentration variation of ozone in the troposphere and stratosphere. This theory involved five reactions:

$$O_2 + h\nu\ (\lambda < 245\ nm) \rightarrow O(^3P) + O(^3P) \quad (1.2)$$

$$O(^3P) + O_2 + M \rightarrow O_3 + M \quad (1.3)$$

$$O(^3P) + O(^3P) + M \rightarrow O_2 + M \quad (1.4)$$

$$O(^3P) + O_3 \rightarrow 2O_2 \quad (1.5)$$

$$O_3 + h\nu\ (\lambda = 220\text{-}315\ nm) \rightarrow O(^1D) + O_2 \quad (1.1)$$

Reactions 1.3, 1.4 and 1.5 are all exothermic and dump heat into the stratosphere. This accounts for the increasing temperature in the stratosphere. Chapman's theory fitted the observed ozone concentration trend quite well but overestimated the actual concentration of ozone indicating that other ozone depleting reactions were taking place. It was later found that chemical species which react with stratospheric ozone can be classified into three groups: hydrogen containing, nitrogen containing and chlorine containing species.

HO_x cycle (x = 0,1,2)

The hydrogen atom is an effective remover of ozone:

$$H + O_3 \rightarrow OH + O_2 \quad (1.6)$$

$$\underline{OH + O \rightarrow H + O_2} \quad (1.7)$$

$$\text{Net: } O_3 + O \rightarrow 2O_2 \quad (1.5)$$

OH and HO_2 also react with ozone:

$$OH + O_3 \rightarrow HO_2 + O_2 \quad (1.8)$$

$$HO_2 + O_3 \rightarrow OH + 2O_2 \quad (1.9)$$

Net: $$2O_3 \rightarrow 3O_2 \quad (1.10)$$

Hydrogen atoms are formed in the stratosphere from the reaction of oxygen atoms with molecular hydrogen while hydroxyl radicals are formed from the reaction of oxygen atoms with molecular hydrogen, water and methane:

$$O(^1D) + H_2 \rightarrow H + OH \quad (1.11)$$

$$O(^1D) + H_2O \rightarrow 2OH \quad (1.12)$$

$$O(^1D) + CH_4 \rightarrow CH_3 + OH \quad (1.13)$$

NO_x cycle (x = 1,2)

NO is formed in the stratosphere from the reaction of oxygen atoms with N_2O. N_2O is emitted into the troposphere from natural microbiological processes in the soil. It is unreactive in the troposphere and diffuses up to the stratosphere where it reacts with $O(^1D)$:

$$O(^1D) + N_2O \rightarrow NO + NO \quad (1.14)$$

$$O(^1D) + N_2O \rightarrow N_2 + O_2 \quad (1.15)$$

The pathway which leads to formation of molecular nitrogen and oxygen (1.15) is the dominant one, particularly between 20 and 40 km [2].

The NO formed then reacts with ozone:

$$NO + O_3 \rightarrow NO_2 + O_2 \quad (1.16)$$

$$\underline{NO_2 + O \rightarrow NO + O_2} \quad (1.17)$$

$$\text{Net: } O_3 + O \rightarrow 2O_2 \quad (1.5)$$

ClO_x cycle (x = 0,1)

Methyl chloride and hydrogen chloride are emitted naturally by wood burning and ocean processes respectively. They are the main biogenic source of chlorine atoms in the stratosphere. Chlorine atoms react rapidly with ozone:

$$Cl + O_3 \rightarrow ClO + O_2 \quad (1.18)$$

$$\underline{ClO + O \rightarrow Cl + O_2} \quad (1.19)$$

$$\text{Net: } O_3 + O \rightarrow 2O_2 \quad (1.5)$$

When the HO_x, NO_x, and ClO_x cycles are incorporated into the Chapman mechanism the resulting ozone concentration versus altitude profile is in excellent agreement with observed data.

Depletion of stratospheric ozone by anthropogenic sources

In 1974 Rowland and Molina [3] proposed that chlorofluorocarbons (CFCs) can lead to the destruction of stratospheric ozone. Chlorofluorocarbons are non-toxic, non-flammable and chemically stable. They have been widely used since the 1930s and have a variety of applications including refrigerants, aerosol propellants and foam-blowing agents. The stability of CFCs means that once emitted to the atmosphere they do not react in the troposphere but are transported to the stratosphere. There, they are photolysed by the shorter wavelength light to release chlorine atoms, eg.

$$CF_2Cl_2 + h\nu\ (\lambda \leq 240\ nm) \rightarrow Cl + CF_2Cl \qquad (1.20)$$

The chlorine atoms then react with ozone as per reactions 1.18 and 1.19. Because the chlorine atom is catalytic, one CFC molecule can lead to the destruction of many ozone molecules.

In 1985 Farman et al. [4] reported a springtime depletion in ozone above Antarctica which had occurred annually since the 1970s. During the Antarctic winter there is no sunlight therefore no ozone is formed. The radicals in the HO_x, NO_x, and ClO_x cycles all revert to inactive forms including H_2O, HNO_3, HCl, CH_3Cl and $ClONO_2$. Strong winds create a vortex in the stratosphere which effectively cuts off the Antarctic stratosphere from the rest of the stratosphere. These conditions cause the temperature to decrease to ~190 K and polar stratospheric clouds containing hydrated HNO_3 crystals

are formed. HCl is adsorbed onto the crystals and a number of heterogeneous reactions can occur including the following:

$$HCl_{(s)} + ClONO_{2(g)} \rightarrow Cl_{2(g)} + HNO_{3(s)} \qquad (1.21)$$

This leads to a build up of Cl_2 and other active chlorine gases such as HOCl in the stratosphere. In October sunlight returns and chlorine atoms are released.

$$Cl_2 + h\nu\ (\lambda > 430\ nm) \rightarrow 2Cl \qquad (1.22)$$

These radicals react rapidly with ozone leading to a massive decrease in stratospheric ozone concentrations. By December the circumpolar vortex has gone and Antarctic ozone can mix with ozone in the rest of the stratosphere. Since measurements of the ozone hole began there has been a steady increase in the amount of ozone lost each spring. Nearly all the ozone between 14 and 18 km now undergoes depletion and the ozone hole lasts longer continuing well into December [5-6]. The Arctic is less susceptible to a polar vortex because it is an ocean surrounded by continents while the Antarctic is a continent surrounded by oceans. However ozone depletion has been observed over the Arctic in recent years [7-9].

1.1.3. The Troposphere

The troposphere comprises two distinct regions. The region of the troposphere nearest the surface of the earth is known as the boundary layer. Its depth varies between about 100m at night and 1000m during the day. Above the boundary layer is the free troposphere. Species with longer atmospheric lifetimes reside here. There is also a contribution from stratospheric components which undergo downward mixing. Table 1.1. shows the average composition of the unpolluted atmosphere along with approximate atmospheric lifetimes. Components with lifetimes of a few days are mainly found in the boundary layer. Those with longer lifetimes mix in the free troposphere and species with lifetimes of a year or more will reach the stratosphere.

When a chemical species is emitted to the troposphere from anthropogenic or biogenic sources it has three possible fates:

1) transportation to the stratosphere
2) wet or dry deposition
3) chemical transformations

Transportation to the stratosphere

Tropospheric components which have an atmospheric lifetime greater than 1 year can be transported to the stratosphere where they may then undergo chemical transformation.

Table 1.1. Average composition of the dry unpolluted atmosphere [10]

Component	Average Concentration / ppm	Approx. Atmospheric Lifetime [a]
N_2	780840	10^6 years
O_2	209460	5000 years
Ar	9340	)
Ne	18	) not
Kr	1.1	) cycled
Xe	0.09	)
CO_2	332	15 years
CO	0.1	65 days
CH_4	1.65	7 years
H_2	0.58	10 years
N_2O	0.33	20 years
O_3	0.01 - 0.1	100 years
NO/NO_2	10^{-6} - 10^{-2}	1 day
NH_3	10^{-4} - 10^{-3}	5 days
SO_2	10^{-5} - 10^{-4}	10 days
HNO_3	10^{-5} - 10^{-3}	1 day

a atmospheric lifetime, τ, is defined as $\tau = \frac{A}{F}$ where

A = global atmospheric burden (Tg)

F = global flux into and out of atmosphere (Tg $year^{-1}$)

Wet or dry deposition

Wet deposition refers to the removal of water soluble species from the atmosphere via precipitation and is significant for NO_x and SO_x. The pollutant can be incorporated into clouds or rain and these processes are known as rainout and washout respectively. Occult desposition occurs when pollutants are deposited onto surfaces by fogwater. This can be a significant loss process for water soluble pollutants as the pollutant concentration in fogwater is higher than in rainwater.

Dry deposition occurs when atmospheric constituents are adsorbed onto soil, water or plant surfaces. Deposition of the species at the surface of the earth leads to a concentration gradient and this drives the process for gases. For particles gravitational settling also occurs. Compounds which undergo dry deposition include SO_2, O_3, CO_2 and SO_3.

Chemical transformations

Chemical constituents can undergo chemical transformation in the troposphere via photolysis and/or reaction with hydroxyl radicals (OH), nitrate radicals (NO_3), ozone (O_3) or chlorine atoms (Cl). For many compounds, particularly saturated organics, reaction with the hydroxyl radical is by far the dominant loss process.

The main source of OH in the natural troposphere is the photolysis of O_3 to give an excited oxygen atom ($O(^1D)$) which can either relax to a ground state oxygen atom ($O(^3P)$) or react with water vapour to give the hydroxyl radical:

$$O_3 + h\nu\ (\lambda = 220\text{-}315\ nm) \rightarrow O(^1D) + O_2 \qquad (1.1)$$

$$O(^1D) + H_2O \rightarrow 2OH \qquad (1.12)$$

$$O(^1D) + M \rightarrow O(^3P) + M \qquad (1.23)$$

Nearly all ground state oxygen atoms will regenerate ozone:

$$O(^3P) + O_2 + M \rightarrow O_3 + M \qquad (1.3)$$

The ozone necessary for production of excited oxygen atoms can be provided by downward mixing of stratospheric ozone. It is also facilitated by the photolysis of NO_2, where present, to produce oxygen atoms which then form ozone via reaction 1.3:

$$NO_2 + h\nu\ (\lambda \leq 400nm) \rightarrow O(^3P) + NO \qquad (1.24)$$

The hydroxyl radical is also formed to a minor extent via reaction of $O(^1D)$ with molecular hydrogen or methane:

$$O(^1D) + H_2 \rightarrow H + OH \quad (1.11)$$

$$O(^1D) + CH_4 \rightarrow CH_3 + OH \quad (1.13)$$

The hydroxyl radical reacts with many trace species in the troposphere including carbon monoxide, sulfur dioxide, hydrogen sulfide, methane, non methane hydrocarbons and nitric oxide. The most significant sinks for OH in the remote troposphere are reaction with methane and carbon monoxide:

$$OH + CH_4 \rightarrow CH_3 + H_2O \quad (1.25)$$

$$OH + CO \rightarrow CO_2 + H \quad (1.26)$$

The radicals formed in reactions 1.25 and 1.26 react with molecular oxygen to form peroxy radicals:

$$CH_3 + O_2 + M \rightarrow CH_3O_2 + M \quad (1.27)$$

$$H + O_2 + M \rightarrow HO_2 + M \quad (1.28)$$

In regions of the troposphere where the mixing ratio of NO is below 30 ppt the peroxy radicals are mainly consumed via reaction with the hydroperoxy radical:

$$CH_3O_2 + HO_2 \rightarrow CH_3OOH + O_2 \quad (1.29)$$

$$HO_2 + HO_2 \rightarrow H_2O_2 + O_2 \quad (1.30)$$

Hydrogen peroxide and methyl hydroperoxide can be removed from the troposphere via wet deposition.

For atmospheric mixing ratios of NO ≥ 30 ppt, NO reacts rapidly with the peroxy radicals to form NO_2 and the corresponding -oxy radicals:

$$HO_2 + NO \rightarrow OH + NO_2 \quad (1.31)$$

$$CH_3O_2 + NO \rightarrow CH_3O + NO_2 \quad (1.32)$$

The methoxy radical produced in reaction 1.32 reacts with molecular oxygen to form formaldehyde:

$$CH_3O + O_2 \rightarrow HCHO + HO_2 \quad (1.33)$$

Formaldehyde is photochemically labile:

$$HCHO + hv \rightarrow H_2 + CO \quad (1.34)$$

$$HCHO + hv \rightarrow H + HCO \quad (1.35)$$

Reaction 1.35 is the dominant pathway and occurs at $\lambda < 338$ nm. Both the HCO and H radicals react with oxygen to yield HO_2:

$$HCO + O_2 \rightarrow CO + HO_2 \quad (1.36)$$

$$H + O_2 + M \rightarrow HO_2 + M \qquad (1.28)$$

The hydroperoxy radical can take part in reactions 1.29, 1.30 and 1.31. Thus a HO_x cycle exists which results in an overall conversion of NO to NO_2. The trace gases, CO and CH_4, are oxidised and the active radical species are regenerated. Larger hydrocarbons are oxidised in a similar manner to methane with the production of a peroxy radical which reacts with NO to form an -oxy radical and NO_2.

$$RO_2 + NO \rightarrow RO + NO_2 \qquad (1.37)$$

1.1.4. Polluted Atmosphere

Photochemical smog was first identified in Los Angeles in the 1940s but now occurs to some extent in most cities. The main contributory factors are sunlight, vehicle exhausts and static air caused by temperature inversions or geological basins. The primary pollutants involved in photochemical smog are NO, CO and hydrocarbons which are emitted from both stationary sources (e.g. stack emissions) and mobile sources (e.g. car exhausts). NO is formed at high temperatures, such as those found in the internal combustion engine.

$$N_2 + O_2 \rightarrow 2NO \qquad (1.38)$$

Carbon monoxide is also a product of combustion and is particularly associated with the petrol engine. The main source of hydrocarbons is the combustion of fossil fuels. One important class of hydrocarbons present in the troposphere is aromatic compounds.

Aromatic hydrocarbons in the atmosphere are classed as air pollutants and can have a direct effect on health as well as contributing to the formation of secondary air pollutants including ozone. Commercial uses of aromatic hydrocarbons include use as solvents and in paint and polymer manufacture. Single ring compounds are constituents of petrol and this is a large source of their release to the atmosphere. Table 1.2. lists some of the aromatic compounds found in petrol.

Reaction with hydroxyl radicals (OH) during the daytime and nitrate radicals (NO_3) during night-time is believed to be the dominant loss process for aromatic compounds in the troposphere [11-12]. Since the reactivity of chlorine atoms is one to two orders of magnitude greater than that of OH radicals towards volatile organic compounds (VOCs) a chlorine atom concentration in the troposphere greater than 10^4 cm^{-3} could provide a significant degradation route for aromatic compounds.

Table 1.2. Aromatic hydrocarbons present in petrol

benzene
methylbenzene (toluene)
1,2-dimethylbenzene (o-xylene)
1,3-dimethylbenzene (m-xylene)
1,4-dimethylbenzene (p-xylene)
1,2,3-trimethylbenzene
1,2,4-trimethylbenzene
1,3,5-trimethylbenzene (mesitylene)
ethylbenzene
1,2-diethylbenzene
1,3-diethylbenzene
1,4-diethylbenzene
1-methyl-2-ethylbenzene (o-ethyltoluene)
1-methyl-3-ethylbenzene (m-ethyltoluene)
1-methyl-4-ethylbenzene (p-ethyltoluene)
n-propylbenzene
n-butylbenzene
i-butylbenzene
t-butylbenzene
1,2-dimethyl-4-ethylbenzene
1,3-dimethyl-4-ethylbenzene
1,4-dimethyl-2-ethylbenzene

Under photochemical smog conditions an important source of OH is photolysis of nitrous acid. HONO is formed from the heterogeneous reaction of water and NO_2:

$$2NO_2 + H_2O \rightarrow HONO + HNO_3 \qquad (1.39)$$

There is a strong diurnal variation in the atmospheric concentrations of HONO with levels increasing at night. After sunrise nitrous acid undergoes photolysis:

$$HONO + h\nu\,(\lambda < 400nm) \rightarrow OH + NO \qquad (1.40)$$

NO and CO enter a chain mechanism with OH resulting in the net formation of NO_2:

$$OH + CO \rightarrow H + CO_2 \qquad (1.26)$$

$$H + O_2 + M \rightarrow HO_2 + M \qquad (1.28)$$

$$HO_2 + NO \rightarrow OH + NO_2 \qquad (1.31)$$

Net: $$NO + O_2 + CO \rightarrow NO_2 + CO_2 \qquad (1.41)$$

NO_2 is responsible for the brown haze which is a distinctive feature of photochemical smog. It undergoes photolysis to form oxygen atoms which then react with molecular oxygen to form ozone:

$$NO_2 + h\nu\ (\lambda \leq 400nm) \rightarrow O(^3P) + NO \quad (1.24)$$

$$O(^3P) + O_2 + M \rightarrow O_3 + M \quad (1.3)$$

Ozone is damaging to plants and affects the respiratory system in humans.

The VOCs emitted are oxidised to form oxygenated products.

$$OH + RCH_3 \rightarrow H_2O + RCH_2 \quad (1.42)$$

$$RCH_2 + O_2 \rightarrow RCH_2O_2 \quad (1.43)$$

$$RCH_2O_2 + NO \rightarrow RCH_2O + NO_2 \quad (1.44)$$

$$RCH_2O + O_2 \rightarrow RCHO + HO_2 \quad (1.45)$$

$$\underline{HO_2 + NO \rightarrow OH + NO_2} \quad (1.31)$$

$$\text{Net}\quad RCH_3 + 2NO + 2O_2 \rightarrow RCHO + NO_2 \quad (1.46)$$

One of the characteristic products of photochemical smog is peroxyacetyl nitrate (PAN).

Its main source is acetaldehyde oxidation:

$$OH + CH_3CHO \rightarrow H_2O + CH_3CO \quad (1.47)$$

$$CH_3CO + O_2 \rightarrow CH_3C(O)O_2 \quad (1.48)$$

$$CH_3C(O)O_2 + NO \rightarrow CH_3C(O)O + NO_2 \quad (1.49)$$

$$CH_3C(O)O + NO_2 \rightarrow CH_3C(O)ONO_2 \quad (1.50)$$

peroxyacetyl nitrate

PAN is hazardous to plants and animals but is important as a sink for reactive nitrogen in the polluted atmosphere. PAN can enter the free troposphere where it is stable due to the low temperatures. When the compound is transported to the boundary layer higher temperatures cause it to decompose releasing NO_2. In this way PAN represents a source of reactive nitrogen in remote atmospheres.

Figure 1.2. shows the concentration of NO, NO_2, O_3 and volatile organic compounds as a function of time during a typical photochemical smog incident. Morning rush hour leads to high levels of NO and hydrocarbons. NO is oxidised to NO_2 which is photolysed by the mid-day sun. NO and O_3 are mutually destructive therefore the conversion of NO must be complete before O_3 can be formed in appreciable quantities. The concentrations of ozone and other secondary pollutants peak in the early afternoon.

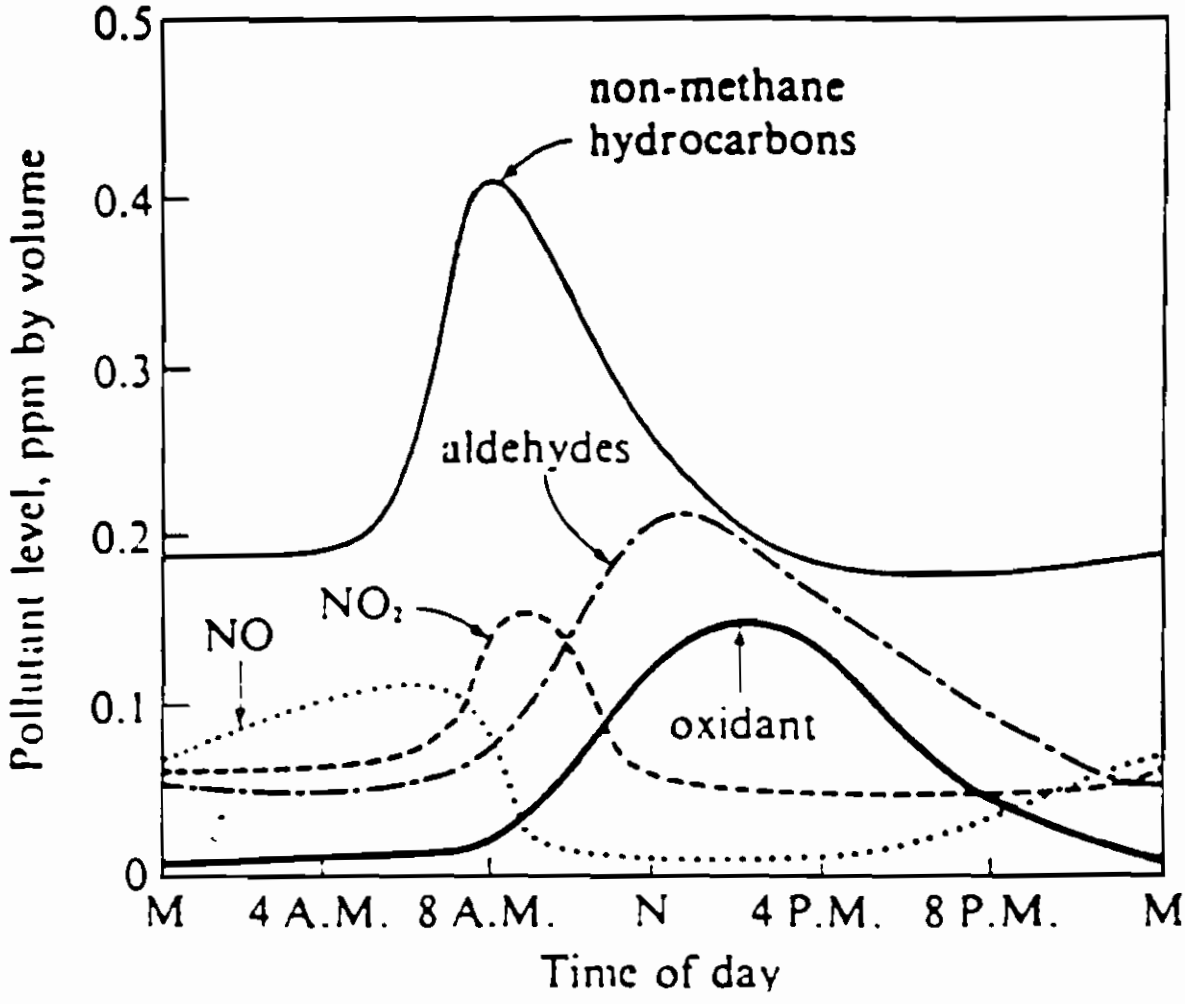

Figure 1.2. Concentrations of pollutants versus time during a photochemical smog incident [13]

1.2. CHLORINE IN THE TROPOSPHERE

1.2.1. Sources of Chlorine in the Troposphere

Chlorine deficits in sea-salt particles

Waves breaking on the surface of the ocean cause the formation of liquid aerosols; when the relative humidity is below the deliquesence point (~75%) evaporation occurs resulting in the formation of solid sea-salt particles with diameters of 0.1-100μm [14]. In the ocean the ratio of chlorine to sodium is approximately 1.8 : 1 [15]. This ratio is considerably decreased in sea-salt particles, particularly in the presence of high NO_x concentrations [15,16], with up to 89% depletion of chlorine observed [16]. In 1941 Cauer [17] found that chloride in sea spray converts to gaseous chlorine compounds. This possibility was the subject of much research during the 1950s [18-23] and the general conclusion was reached that most of the chlorine deficit observed in sea-salt particles was due to the volatilisation of HCl. This can occur when the pH of the marine particle (normally between 7 and 9 [16]) is less than 3 due to the adsorption of acids [16,24]:

$$HNO_{3(p)} + NaCl_{(p)} \rightarrow HCl_{(g)} + NaNO_{3(p)} \quad (1.51)$$

$$H_2SO_{4(p)} + 2NaCl_{(p)} \rightarrow 2HCl_{(g)} + Na_2SO_{4(p)} \quad (1.52)$$

g and p indicate gaseous and particle phase respectively.

HCl is a potential source of chlorine atoms via reaction with hydroxyl radicals in the gas phase:

$$HCl + OH \rightarrow H_2O + Cl \qquad (1.53)$$

The main loss process for HCl in the troposphere is via wet and dry deposition [15,25] therefore reaction 1.53 is unlikely to occur to any significant extent. HCl can also be re-incorporated into particulate matter with an estimated time scale of the order of 10 minutes for scavenging of HCl by sea-salt aerosol [16].

Laboratory studies of sea-salt reactions

A number of laboratory studies have been carried out, particularly since the late 1980s, investigating the possibility that gaseous chlorine compounds, other than HCl, are released from sea-salt particles and that these gases could be a source of chlorine atoms in the troposphere [26-33]. Finlayson-Pitts et al. [26] studied the reaction of $ClONO_2$ and N_2O_5 with NaCl. For the former reaction, mixtures of $ClONO_2$ in helium were flowed through a cylindrical cell packed with NaCl and then into a mass spectrometer. The N_2O_5 experiments were carried out by placing dilulte mixtures of N_2O_5 in 1 atm. air into a reaction bulb containing ~ 100g of NaCl. The reactants were allowed to mix in the dark for one hour before FTIR analysis of the reacted gas mixture.

The investigators found that gaseous $ClONO_2$ and N_2O_5 react with dry NaCl to produce Cl_2 and $ClNO_2$ respectively, both of which photolyse at $\lambda > 350$ nm to give chlorine atoms:

$$NaCl_{(p)} + ClONO_{2(g)} \rightarrow Cl_{2(g)} + NaNO_{3(p)} \quad (1.54)$$

$$Cl_2 + h\nu \rightarrow 2Cl \quad (1.22)$$

$$NaCl_{(p)} + N_2O_{5(g)} \rightarrow ClNO_{2(g)} + NaNO_{3(p)} \quad (1.55)$$

$$ClNO_2 + h\nu \rightarrow Cl + NO_2 \quad (1.56)$$

A reaction mechanism was proposed which suggests that reactions 1.54 and 1.55 may be faster at lower temperatures. These reactions, therefore, would be particularly significant at higher latitudes. Behnke et al. [33] carried out aerosol smog chamber and wetted-wall flow tube experiments on the reaction of N_2O_5 with liquid NaCl aerosols and bulk NaCl solutions. The results showed that the uptake of N_2O_5 by NaCl solutions to produce $ClNO_2$ is a very efficient process even for very dilute NaCl solutions and thus is a very likely source of $ClNO_2$ and hence chlorine atoms in the marine boundary layer.

The reaction of sea-salt with NO_2 has been studied in detail [27-29,31-32] by techniques including diffuse reflectance infrared Fourier transform spectroscopy (DRIFTS) [27,28] and electron paramagnetic resonance (EPR) [29]. All investigators agree that this reaction results in the formation of sodium nitrate and NOCl:

$$NaCl_{(p)} + 2NO_{2(g)} \rightarrow NOCl_{(g)} + NaNO_{3(p)} \quad (1.57)$$

NOCl can then undergoes photolysis to produce chlorine atoms:

$$NOCl + h\nu\ (\lambda = 280\text{-}400\ nm) \rightarrow Cl + NO \quad (1.58)$$

However, there is general agreement between all the researchers that reaction 1.57 is too slow under ambient conditions to contribute to the tropospheric concentration of chlorine atoms.

As well as releasing photolysable chlorine gases reactions 1.54, 1.55 and 1.57 result in the formation of sodium nitrate. It was suggested [26] that once the NaCl at the surface of the sea-salt particles had reacted with NO_x the nitrate formed would prevent any further reactions between NO_x and chloride in the bulk particle. More recent studies have shown that this is not the case [24,29,34-35] since in the presence of water the nitrate recrystallises into separated microcrystallites of $NaNO_3$ exposing fresh layers of NaCl for reaction. This occurs at relative humidities less than the deliquesence point [34].

Keene et al. [16] measured the concentration of chloride, nitrate and sulphate anions on sea-salt particles. They found that chloride deficits in the particles were enhanced at night as would be expected if photolysable inorganic chlorine containing gases are being

released. These results led the authors to conclude that reactions 1.51, 1.52, 1.54, 1.55 and 1.57 could not account for all of the chlorine deficit found. They hypothesised a photochemical mechanism for the formation of Cl_2 initiated by ozone which was originally suggested by Behnke & Zetzsch [36]:

$$O_3 + h\nu\ (\lambda = 220\text{-}315\ nm) \rightarrow O(^1D) + O_2 \quad (1.1)$$

$$O(^1D)_{(g)} + H_2O_{(g)} \rightarrow 2\cdot OH_{(g)} \quad (1.11)$$

$$\cdot OH_{(g)} \rightarrow \cdot OH_{(p)} \quad (1.59)$$

$$\cdot OH_{(p)} + Cl^-_{(p)} \rightarrow \cdot ClOH^-_{(p)} \quad (1.60)$$

$$\cdot ClOH^-_{(p)} \leftrightarrow {}^-OH_{(p)} + Cl\cdot_{(p)} \quad (1.61)$$

$$Cl\cdot_{(p)} + Cl^-_{(p)} \rightarrow \cdot Cl_2^-{}_{(p)} \quad (1.62)$$

$$\cdot Cl_2^-{}_{(p)} + \cdot Cl_2^-{}_{(p)} \rightarrow Cl_{2(g)} + 2Cl^- \quad (1.63)$$

Zetzsch and Behnke [30,36] observed that Cl_2 is also formed in the dark in the presence of NaCl and O_3. They proposed a direct surface reaction between O_3 and Cl^-:

$$2Cl^- + O_{3(g)} \xrightarrow{H2O} Cl_{2(g)} + 2OH^- + O_{2(g)} \quad (1.64)$$

HOCl is another inorganic chlorine containing gas which is easily photolysed to give chlorine atoms. It is formed by the heterogeneous hydrolysis of chlorine nitrate:

$$ClONO_{2(g)} + H_2O_{(p)} \rightarrow HOCl_{(g)} + HNO_{3(p)} \quad (1.65)$$

$$HOCl + h\nu \rightarrow Cl + OH \quad (1.66)$$

Reaction 1.65 has been studied in relation to the stratosphere [37] but similar reactions are likely to occur in the troposphere, particularly at lower temperatures. The heterogeneous reactions of chlorine nitrate (reactions 1.54 and 1.65) have first order rate constants in the range 10^{-5} to 10^{-3} s^{-1} [38] and compete with the photolysis of chlorine nitrate (see table 1.3., reaction 1.67).

1.2.2. Concentrations of Chlorine Atoms in the Troposphere

There is an increasing body of evidence which supports the presence of significant amounts of chlorine atoms in the troposphere. However, results of other studies have been published which are in conflict with this. Table 1.4. summarises estimated chlorine atom concentrations in the marine boundary layer (MBL).

Non-Arctic studies

Modelling studies carried out by Singh and Kasting [38] showed that 20 - 40% of the total oxidation of non-methane hydrocarbons (NMHCs) is caused by chlorine atoms. From this they estimated a chlorine atom concentration of 10^3 cm^{-3} in the marine troposphere. This estimate is likely to be too low as the authors disregarded heterogeneous chemistry and assumed that the reaction of HCl with hydroxyl radicals was the main source of chlorine atoms.

Table 1.3. Photolysis rate constants for reactions which yield chlorine atoms

Reaction		Rate constant / s^{-1} [a]
$Cl_2 + h\nu \rightarrow 2Cl$	(1.22)	1.76×10^{-3}
$HOCl + h\nu \rightarrow Cl + OH$	(1.66)	1.92×10^{-4}
$NOCl + h\nu \rightarrow Cl + NO$	(1.58)	1.42×10^{-3}
$ClNO_2 + h\nu \rightarrow Cl + NO_2$	(1.56)	3.32×10^{-3}
$ClONO_2 + h\nu \rightarrow Cl + NO_2 + O$	(1.67)	4.79×10^{-5}

a Photolysis rates are calculated using the rate constants and cross sections of DeMore et al. [39] and the solar fluxes from WMO [40]. The rates are the diurnally-averaged value at 19.5 km for a solar zenith angle of 50°.

Table 1.4. Cl atom concentrations in the marine boundary layer

Concentration/cm^3	Location	Remarks	Reference
10^3	Global Troposphere	modelled assuming 1000pptv HCl and reaction with OH	[38]
6×10^3 - 1×10^6	North Atlantic	modelled based on Cl^- deficits	[16]
0.1 - 4×10^3	Global Troposphere	modelled based on reaction of NaCl with N_2O_5 only	[30]
$<10^4$ - 10^5	Florida, U.S.A.	modelled based on measured HCl^* and Cl^*	[41]
4×10^3 - 8×10^4	Alert, Canada	inferred from NMHC data	[42]
2×10^4 - 8×10^5	Tropical Pacific	inferred from NMHC data	[43]
10^3 (upper limit)	Marine Boundary Layer	inferred from NMHC data	[44]
<5 - 15×10^3 (upper limit)	Marine Boundary Layer	inferred from NMHC data	[45]
10^4	Alert, Canada	modelled based on measured $Cl_{2(p)}$	[46]
10^4	North Atlantic	inferred from NMHC data	[47]

HCl^* includes HCl, $ClONO_2$, $ClNO_2$ and NOCl

Cl_2^* includes Cl_2 and HOCl

Modelling studies were also carried out by Keene et al. [16] who included a number of chlorine chemistry scenarios in their model. Their minimum chlorine atom concentration of 10^3 cm^{-3} corresponded to the inclusion of reaction of HCl with hydroxyl radicals only while their upper limit of [Cl] = 10^6 cm^{-3} included the reactions HCl + OH (1.53), $ClONO_2$ + Cl^- (1.54) and O_3 + Cl^- (1.64).

Pszenny et al. [41] used a tandem mist chamber to measure concentrations of HCl^* (including HCl, $ClONO_2$, $ClNO_2$ and NOCl) and Cl_2^* (including Cl_2 and HOCl) in the marine troposphere. By applying a photochemical model to the measured values of $[Cl_2^*]$ the authors calculated a chlorine atom concentration in the MBL of 10^4 - 10^5 atoms cm^{-3}. A possible source of error is that the measured values of $[HCl^*]$ includes photolysable chlorine ($ClONO_2$, $ClNO_2$ and NOCl) and this is not included in the model. The results of this measurement study showed that after sunrise $[Cl_2^*]$ decreased while $[HCl^*]$ increased and the reverse happened at night. This is consistent with levels of photolysable chorine ($Cl_{2(p)}$) building up at night due to heterogeneous reactions and releasing chlorine atoms during the day. The chlorine atoms then react with NMHCs forming HCl which explains the observed increase in $[HCl^*]$. Their results for the decline in $[Cl_2^*]$ after dawn suggests a lifetime due to photolysis of a few hours implying that HOCl is the dominant precursor rather than Cl_2 since HOCl has a longer photolysis lifetime than Cl_2.

A similar study by Spicer et al. [48] used an atmospheric-pressure chemical ionization tandem mass spectrometer to measure concentrations of Cl_2 in air originating from the marine boundary layer of the North Atlantic. Their results were in the same range as Pszenny et al. [41] and they also noticed a build-up of Cl_2 at night indicating the existence of a non-photolytic mechanism for Cl_2 production.

Singh et al. [43] measured the concentrations of C_2H_6, C_3H_8, C_2H_2, C_2Cl_4 and $(CH_3)_2S$ in the marine boundary layer of the tropical Pacific Ocean. All these compounds react much faster with chlorine atoms than with hydroxyl radicals ($k_{Cl} \geq 60\ k_{OH}$). By comparing concentrations of the organics measured in the daytime with those measured during the night the authors inferred a chlorine atom concentration of 10^4 - 10^5 cm^{-3}.

Wingenter et al. [47] monitored the decrease in concentration with respect to time of five C_2-C_5 non-methane hydrocarbons and two halocarbons in a parcel of air in the marine boundary layer of the North Atlantic. The rate constants for reaction of these compounds with chlorine atoms is different to the rate constants for their reaction with hydroxyl radicals therefore the decrease in concentration of the hydrocarbons and halocarbons depends on the concentration of chlorine atoms and hydroxyl radicals in the MBL. From their results the authors calculated a chlorine atom concentration of 10^4 cm^{-3} in the marine boundary layer.

A number of studies [44,45] found evidence for low concentrations of chlorine atoms in the troposphere. Singh et al. [45] analysed the atmospheric budget of tetrachloroethene. Since the main sources of atmospheric C_2Cl_4 are anthropogenic, data is available for the global emission rates. Using modelling studies, the authors compared the amount of C_2Cl_4 emitted with the amount measured in the atmosphere and found that almost all the depletion of C_2Cl_4 observed could be accounted for by reaction with hydroxyl radicals. The authors concluded that the concentration of chlorine atoms in the atmosphere is low and calculated an upper limit in the MBL $\leq 5 - 15 \times 10^3$ cm^{-3}. Possible sources of error in the study could include inaccurate values for C_2Cl_4 emissions and OH concentrations and the possibility of an oceanic source of C_2Cl_4.

Rudolph et al. [44] performed similar calculations with the budgets of tetrachlorethene and ethane. Their results yielded an upper limit of 10^3 cm^{-3} for the concentration of chlorine atoms in the marine boundary layer. The results for C_2Cl_4 were quite different to those for C_2H_6 and the overall results had a large uncertainty. Both studies [44,45] used limited sets of data. The studies of Singh et al. [43] and Jobson et al. [42] which looked at a larger number of hydrocarbons probably give more accurate estimates for chlorine atom concentrations in the troposphere.

Arctic studies

A number of monitoring studies [42,46,49,50] have been carried out in the Arctic region due to the long period of darkness during the winter when concentrations of photolysable chlorine would be expected to build up followed by a decrease after sunrise. Impey et al. [46] found this to be the case when they measured photolysable chlorine (assumed to be mainly Cl_2 and HOCl) in the Arctic using a photoactive halogen detector. The results of the study suggested that chlorine atoms were present in the marine boundary layer in concentrations of about 10^4 cm^{-3}. The sampling period represented the transition from 24 hour darkness to 24 hour daylight. As expected the concentration of photolysable chlorine decreased continually after sunrise until it was below the detection limit of the instrument. The diurnal profile, however, showed a late morning maximum and a minimum near midnight which does not indicate the presence of a rapidly photolysable species. The authors suggested that this implies a photo-induced source as well as a dark mechanism for $Cl_{2(p)}$ production which agrees with the findings of Keene et al. [16] and Behnke & Zetzsch [36].

Jobson et al. [42] measured a number of C_2-C_6 hydrocarbons, including benzene, in the Arctic MBL from January (24 hour darkness) to April (24 hour sunlight). During the winter when there was no sunlight they found that the concentrations of the hydrocarbons correlated with those of methane and throughout the sampling period the decrease in hydrocarbon concentrations was generally consistent with hydroxyl radical chemistry. In the Arctic spring the tropospheric ozone concentration occasionally drops

dramatically and three such episodes were observed during this study. During these periods of ozone depletion the concentrations of most of the hydrocarbons also showed a substantial decrease. These concentration changes showed excellent correlation with chlorine atom rate constants giving strong evidence that chlorine atoms were present at concentrations between 4×10^3 - 8×10^4 cm^{-3}. The loss of ozone was purported to be due to the presence of bromine atoms at concentrations of 10^6 - 10^7 cm^{-3}, a finding which is consistent with the data of Impey et al. [46].

Shepson et al. [49] measured the concentrations of methanal, ethanal and propanone in the Arctic spring. They observed an increase in concentration of the carbonyl compounds during low ozone episodes. Bromine atoms, which were assumed to be responsible for the ozone depletion, represent a path for removal of the carbonyl compounds, and hence could not be responsible for the observed concentration increase. Chlorine atoms lead to both the production and loss of carbonyl compounds. Modelling studies carried out by the authors showed that chlorine atom concentrations of the order of 5×10^4 cm^{-3} would result in the efficient production of the carbonyl compounds but not at the high concentrations found in the study. They noted that the carbonyl concentration is inversely proportional to the bromine atom/chlorine atom ratio but imposed a lower limit of [Br]/[Cl]=1000 after Jobson et al. [42] which gave an upper limit of [Cl] = 5×10^4 atoms cm^{-3}. Their model implies that higher concentrations of chlorine atoms would explain their results.

Wegner et al. [50] measured the concentration of HCl and HCHO at a site in Northern Sweden and found that the concentration of both compounds was much higher in air which originated from polar maritime regions than that which originated from midlatitudinal maritime regions while continental midlatitudinal air had the lowest concentrations of all. A strong positive correlation between the two species was also found. The results of this study are consistent with the presence of chlorine atoms in the marine boundary layer as chlorine atoms are responsible for the production of HCHO and HCl.

Role of Chlorine Atoms in Air Pollution

The heterogeneous reactions of NO_x with NaCl is particularly relevant in the polluted marine atmosphere and hence has implications for many large coastal cities around the world. In addition sea-salt particles can be transported inland and have been identified at distances up to 900 km from the sea [51]. NaCl particles can also be released from oil wells; large amounts were measured after the oil well burning in Kuwait [52-54].

Chlorine atoms can have an impact on the concentration of secondary air pollutants. Singh and Kasting [38] found that, while chlorine atoms in the troposphere had little effect on PAN concentrations as they are involved in both its production and its loss, removal of ozone from the atmosphere via direct reaction can occur:

$$Cl + O_3 \rightarrow ClO + O_2 \qquad (1.18)$$

However in polluted environments the increased supply of peroxy radicals from the reaction of NMHCs with chlorine atoms would increase the ozone concentration. The net effect of chlorine chemistry is to decrease the concentration of ozone at NO_x concentrations below about 20 pptv and to stimulate ozone production at higher NO_x concentrations [41]. In the remote marine boundary layer, where the concentration of NO_x is low, O_3 may also be removed by adsorption onto sea-salt particles.

Keene et al. [16] suggest that this is the reason for low ozone concentrations measured in the MBL. Singh et al. [43] concluded that the effect of chlorine atoms on loss of ozone would only be significant at concentrations of 10^6 cm^{-3}.

Hov [55] examined an industrial area where molecular chlorine was emitted as a pollutant along with hydrocarbons, SO_2, NO_x and CO. It was found that the presence of chlorine atoms (10^6 cm^{-3}) caused a large increase in the concentration of OH and HO_2 radicals, aldehydes and peroxyacetylnitrate (PAN) and a smaller increase in ozone. The concentration of NO_x and SO_2 also increased causing very rapid nitric acid and sulphate formation. In the absence of chlorine less than 1% of the hydrocarbons present were degraded within an hour whereas with chlorine concentrations of 10^6 atoms cm^{-3} up to 70% of the hydrocarbons were removed in the same time period. Modelling studies by Hov [55] showed that if chlorine emissions were removed the concentration of PAN decreased by a factor of 30 demonstrating that the presence of chlorine atoms has a large effect on the formation of secondary pollutants.

Chapter 2

Kinetic Studies on the Reactions of Chlorine Atoms with Aromatic Compounds

2.1. INTRODUCTION

2.1.1. Experimental techniques for kinetic analyses

Rate constants for gas phase reactions are determined using either the relative rate method or an absolute technique. For kinetic analyses, the majority of atmospherically relevant gas phase reactions studied are simple bimolecular reactions in the form:

$$A + B \xrightarrow{k} \text{products} \qquad (2.1)$$

where A is the reactive atom, radical or molecule (e.g. OH, Cl, NO_3, O_3)

B is the stable species (e.g. VOCs, NO, NO_2, SO_2)

k is the rate constant for the reaction

The relative rate technique involves measuring the loss of the more stable species (B in eqn. 2.1) relative to the loss of a reference compound. The absolute rate constant for the reaction of the reference compound with the reactive species (A in eqn. 2.1) must be known.

The reactant substrate and reference compound react with the reactive species, A, thus:

$$A + \text{reactant substrate} \xrightarrow{k_S} \text{products} \qquad (2.2)$$

$$A + \text{reference compound} \xrightarrow{k_r} \text{products} \qquad (2.3)$$

Assuming that the loss process for the reactant and reference compounds is solely via reactions 2.2 and 2.3, then

$$-d[\text{reactant substrate}]/dt = k_s[A][\text{reactant substrate}]$$

$$-d[\text{reference compound}]/dt = k_r[A][\text{reference compound}]$$

where k_s and k_r are the rate constants for reactions 2.2 and 2.3 respectively.

Rearranging gives

$$-d \ln[\text{reactant substrate}] = k_s[A]\,dt$$

$$-d \ln[\text{reference compound}] = k_r[A]\,dt$$

Integrating these equations gives

$$-\{\ln[\text{reactant substrate}]_t - \ln[\text{reactant substrate}]_{t0}\} = k_s[A]t$$

$$-\{\ln[\text{reference compound}]_t - \ln[\text{reference compound}]_{t0}\} = k_r[A]t$$

Eliminating [A] and rearranging gives

$$\ln\left[\frac{[\text{reactant substrate}]_{t_0}}{[\text{reactant substrate}]_t}\right] = \frac{k_S}{k_r} \ln\left[\frac{[\text{reference compound}]_{t_0}}{[\text{reference compound}]_t}\right] \qquad \text{I}$$

where [reactant substrate]$_{t0}$ and [reference compound]$_{t0}$, and [reactant substrate]$_t$ and [reference compound]$_t$ are the concentrations of the reactant substrate and reference compound at times t_0 and t respectively. Hence, a plot of ln ([reactant substrate]$_{t0}$/[reactant substrate]$_t$) against ln ([reference compound]$_{t0}$/[reference compound]$_t$) should give a straight line of slope k_s/k_r with zero intercept.

When using the relative rate technique it is assumed that the only loss process for the reactant substrate and reference compound is via reaction with A and this assumption must be verified. However, if other loss processes exist that are quantifiable (eg. photolysis) the relative rate technique can still be employed. The loss of the reactant substrate and reference compound is usually monitored using gas chromatography or infrared spectroscopy.

Determination of an absolute rate constant involves measuring either the loss of a reactant or the formation of a product with respect to time. The techniques used in the study of atmospherically relevant gas phase reactions involve measuring the loss of either the reactive species (reactant A in eqn. 2.1) or the substrate (reactant B in eqn. 2.1) under pseudo-first-order conditions where the concentration of the other reactant is

in large excess. The rate of disappearance of the reactant with the lowest concentration follows a simple exponential rate law:

$$[A]_t = [A]_0 \exp(-k't) \qquad \text{where } k' = k[B] + k_0$$

where k' is the pseudo first order rate constant,

k is the bimolecular rate constant for the reaction

[A] is the concentration of the reactant with lower concentration

[B] is the concentration of the reactant in excess

Most absolute rate constants are measured using either a fast flow discharge system (FFDS) or a flash photolysis system. In a fast flow system an inert gas (e.g. He or Ar) flows at speeds of ~1000 cm s^{-1} through a flow tube of diameter 2 - 5 cm and length 1 - 3 m. At the end of the tube is a detector to monitor the concentration of the more reactive species, A. The reactants, A and B, are introduced at a known distance from the detector and this distance is varied by means of a moveable injector. Thus the decay of A with time is monitored and the rate constant can then be calculated.

In a FFDS system the reactive species, A, is generated by means of a microwave discharge. Hydrogen and oxygen atoms can be produced by direct discharging of the corresponding diatomic molecules, however, this can result in a mixture of atoms and molecules in different excited states. This problem is avoided by using an indirect discharge method. For example, ground state oxygen atoms can be produced by the

microwave discharge of molecular nitrogen to form nitrogen atoms which are then reacted with NO:

$$N_2 \xrightarrow{\lambda = 1\text{-}50\text{cm}} 2N \qquad (2.4)$$

$$N + NO \longrightarrow N_2 + O(^3P) \qquad (2.5)$$

Hydroxyl radicals can be produced in a number of indirect ways including the reaction of hydrogen atoms with NO_2 (2.6) and the reaction of fluorine atoms with water (2.7). In both cases the reactant atom is produced by microwave discharge of the parent molecule:

$$H + NO_2 \rightarrow OH + NO \qquad (2.6)$$

$$F + H_2O \rightarrow OH + HF \qquad (2.7)$$

The decay of the reactive species is followed as a function of time by monitoring some physical property which is proportional to concentration. A variety of detection systems are employed, the most popular being resonance fluorescence, laser induced fluorescence, laser magnetic resonance and mass spectrometry.

Resonance fluorescence is used when the reactive species is an atom (e.g., H, N, O, F, Cl, Br) although it can also be used for some molecular species, e.g. OH [56]. In a resonance lamp the diatomic molecule is passed through a microwave discharge which causes some of the molecules to dissociate. Some of the resulting atoms are electronically excited and fluoresce. This light is absorbed by atoms of the same species

in the flow tube which then also fluoresce. A photomultiplier tube measures the intensity of this fluorescence and hence the relative concentration of the atomic species.

Laser induced fluorescence is similar to resonance fluorescence and is used to measure the concentration of molecular radical species. It was first used to measure the hydroxyl radical in 1977 by Lengel et al. [57]. The species being measured is excited using a dye laser, the laser being tuned so that the radical species undergoes one particular rovibrational transition resulting in greater selectivity. Fluorescence then occurs and the relative concentration of the radical species can be found.

Laser magnetic resonance can be used to detect species with a magnetic moment which includes most radicals. The technique is based on the Zeeman effect: a magnetic field causes shifts in the energy levels of the radical so that it absorbs infrared energy produced by a CO_2 laser. When the absorption is known the concentration can be found from the Beer-Lambert law.

A number of reactive species, particularly the more stable molecules, can be monitored using conventional mass spectrometry. Difficulties arise when attempting to measure concentrations of atoms and radicals due to fragmentation in the electron impact ioniser. Jones and Bayes [58] found that using photons to cause ionisation avoids these problems, a technique known as photoionisation mass spectrometry.

The technique of flash photolysis was developed by Norrish and Porter in the 1940s [59]. It involves using a flash of light to generate the reactive species whose concentration is then monitored as a function of time. The photolysis chamber contains the premixed reactant and radical precursor and thererfore the mixing time is zero; an advantage over FFDS. In order to avoid the accumulation of photolysis or reaction products and to minimize any uncertainties in reactant concentration arising from adsorption on the reactor walls, experiments are carried out under slow flow conditions. The flow rate is such that each photolysis flash encounters a fresh reaction mixture. Some examples of precursors are Cl_2 for Cl atoms, CH_3ONO for CH_3O radicals and CH_3COCH_3 for CH_3 radicals. A variety of precursors have been used to produce OH radicals including H_2O [60], H_2O_2 [61], HNO_3 [61,62], O_3-H_2O [63] and NO_2-H_2 [64]. Excimer lasers [61] or frequency quadrupled Nd:YAG lasers [63] are normally used to provide the photolysis light. These supply short pulses of monochromatic radiation with a choice of lasing wavelengths. The reactive species can also be generated by a short pulse of high energy electrons, a technique known as pulse radiolysis. The main methods used for detection of the reactive species in flash photolysis systems are resonance fluorescence, laser-induced fluorescence and resonance absorption.

2.1.2. PREVIOUS KINETIC STUDIES ON REACTIONS OF CHLORINE ATOMS WITH VOLATILE ORGANIC COMPOUNDS

To date most of the work carried out on the reactions of chlorine atoms with volatile organic compounds has been related to stratospheric chemistry. The rate constant for the reaction of chlorine and methane has been particularly well documented using both absolute techniques [65-77] and the relative rate method [66,77-82]. The reaction proceeds via abstraction of a hydrogen atom from methane to form HCl.

$$CH_4 + Cl \rightarrow HCl + CH_3 \qquad (2.8)$$

Some of this HCl can diffuse to the troposphere where it undergoes wet and dry deposition thus providing a sink for stratospheric chlorine atoms.

CH_3Cl is the most abundant natural VOC and is present in the stratosphere. It was therefore considered as a potential sink for stratospheric chlorine atoms. The kinetics of the reactions of chlorine atoms with halogenated methanes were investigated in a number of studies [66,73,82-84]. This progressed to the study of the reactions of chlorine atoms with halogenated ethanes, particularly as these compounds were considered as replacement compounds for CFCs [85].

As interest in the gas phase chemistry of chlorine atoms grew the kinetics of the reactions of chlorine with many volatile organic compounds were studied including alkanes [66,86-93], alkenes and alkynes [88,94-97], aromatic compounds [88,95,98-101] halogenated compounds [73,85,87-89,92,95,102-114], nitrogen containing compounds [115-119], and oxygenated compounds [90,104,105,115,117,120-129].

The available rate data for reactions of chlorine atoms with aromatic compounds are shown in Table 2.1. together with kinetic data for the reactions of chlorine atoms with alkanes and alkenes.

Table 2.1. Rate constants for reaction of chlorine atoms with alkanes, alkenes and aromatic compounds at 298 K

Substrate	$10^{11} \times k_{Cl}$ cm^3 $molecule^{-1}s^{-1}$	Technique	Literature Reference
alkanes			
methane	0.01	Review	Atkinson [130]
	0.01 ± 0.001	Review	DeMore et al. [131]
	0.0094 ± 0.004	FFD-RF	Beichert et al. [66]
	0.0099 ± 0.004	TFT-RF	Seeley et al. [132]
	0.0093 ± 0.009	LP-IR	Pilgrim et al. [133]
ethane	5.9	Review	Atkinson [130]
	5.7 ± 0.6	Review	De More et al. [131]
	5.53 ± 0.21	FFD-RF	Beichert et al. [66]
	5.5 ± 0.2	LP-IR	Pilgrim et al. [133]
	5.75 ± 0.20	FP-RF	Tyndall et al. [87]
propane	13.7	Review	Atkinson [130]
	14 ± 1.8	Review	De More et al. [131]
	12.3 ± 1.0	FFD-RF	Beichert et al. [66]
	13.8 ± 0.2	LP-IR	Pilgrim et al. [133]
	13.7 ± 0.7	RR	Tyndall et al. [87]
n-butane	21.8	Review	Atkinson [130]
	22.3 ± 3.29	DF-RF	Lewis et al. [86]
	21.5 ± 0.15	FP-RF	Tyndall et al. [87]
	21.9 ± 1.0	RR	Tyndall et al. [87]
	21.1 ± 1.8	FFD-RF	Beichert et al. [66]
i-butane	14.3	Review	Atkinson [130]
	15.1 ± 0.9	RR	Wallington et al. [90]
	14.6 ± 0.6	DF-RF	Lewis et al. [86]
	13.7 ± 0.2	RR	Atkinson & Aschmann [88]
	14.0 ± 0.8	FFD-RF	Beichert et al. [66]
	13.0 ± 0.1	RR	Hooshiyar & Niki [134]

Table 2.1. continued

n-pentane	28	Review	Atkinson [130]
	31.0 ± 1.6	RR	Wallington et al. [90]
	25.2 ± 1.2	RR	Atkinson & Aschmann [88]
	25.0 ± 0.2	RR	Hooshiyar & Niki [134]
i-pentane	22	Review	Atkinson [130]
	20.3 ± 0.8	RR	Atkinson & Aschmann [88]
	19.6 ± 0.2	RR	Hooshiyar & Niki [134]
neopentane	11	Review	Atkinson [130]
	11.0 ± 0.3	RR	Atkinson & Aschmann [88]
n-hexane	34	Review	Atkinson [130]
	34.5 ± 2.3	RR	Wallington et al. [90]
	30.3 ± 0.6	RR	Atkinson & Aschmann [88]
	30.5 ± 0.4	RR	Hooshiyar & Niki [134]
cyclohexane	35	Review	Atkinson [130]
	36.1 ± 1.5	RR	Wallington et al. [90]
	31.1 ± 1.4	RR	Atkinson & Aschmann [88]
	30.8 ± 1.2	RR	Aschmann & Atkinson [91]
n-heptane	39	Review	Atkinson [130]
	34.1 ± 1.2	RR	Atkinson & Aschmann [88]
	36.5 ± 0.6	RR	Hooshiyar & Niki [134]
n-octane	46	Review	Atkinson [130]
	40.5 ± 1.2	RR	Aschmann & Atkinson [91]
	40.9 ± 1.2	RR	Hooshiyar & Niki [134]
n-nonane	48	Review	Atkinson [130]
	42.9 ± 1.2	RR	Aschmann & Atkinson [91]
n-decane	55	Review	Atkinson [130]
	48.7 ± 1.8	RR	Aschmann & Atkinson [91]

Table 2.1. continued

alkenes			
ethene	10.7	Review	Atkinson [130]
	10.6 ± 1.3	RR	Atkinson & Aschmann [88]
	12.1 ± 0.7	RR	Wallington et al. [95]
propene	28	Review	Atkinson [130]
	10.6 ± 1.3	RR	Atkinson & Aschmann [88]
	12.1 ± 0.7	RR	Wallington et al. [95]
1,2-propadiene	42	Review	Atkinson [130]
	43.8 ± 2.6	RR	Wallington et al. [95]
aromatic hydrocarbons			
benzene	1.5 ± 0.9	RR	Atkinson et al. [88]
	< 0.4	RR	Wallington et al. [95]
	< 0.00005	RR	Nozière et al. [98]
	0.0089 ± 0.0016	RR	Berho et al. [99]
	0.00013 ± 0.00003	RR	Shi et al. [100]
toluene	5.89 ± 0.36	RR	Atkinson et al. [88]
	5.59 ± 0.28	RR	Wallington et al. [95]
	5.81 ± 1.81	RR	Bartels et al. [135]
	5.65 ± 0.60	PR-UVS	Markert et al. [101]
	6.1 ± 0.2	RR	Nozière et al. [98]
	5.9 ± 0.5	RR	Shi et al. [100]
o-xylene	12.0 ± 0.9	RR	Wallington et al. [95]
	15 ± 1	RR	Shi et al. [100]
m-xylene	12.0 ± 1.4	RR	Wallington et al. [95]
	14 ± 1	RR	Shi et al. [100]
p-xylene	13.3 ± 0.8	RR	Wallington et al. [95]
	15 ± 1	RR	Shi et al. [100]

Table 2.1. notes

FFD-RF determined using the absolute technique of fast flow discharge with resonance fluorescence at 1 Torr pressure.

TFT-RF determined using the absolute technique of turbulent flow tube with resonance fluorescence at ~ 60 Torr pressure.

LP-IR determined using the absolute technique of laser photolysis with continuous wave infrared long-path absorption at 10 Torr pressure.

FP-RF determined using the absolute technique of flash photolysis-resonance fluorescence at 15 - 60 Torr pressure.

RR determined from relative rate measurements at 1 atm. pressure.

DF-RF determined using the absolute technique of low pressure discharge-flow-resonance fluorescence.

PR-UVS determined using the absolute technique of pulse radiolysis combined with time-resolved ultraviolet spectroscopy at 1 atm. pressure.

DF-MS determined using the absolute technique of discharge flow combined with mass spectrometry

The first kinetic data for the reactions of chlorine atoms with aromatic hydrocarbons was reported by Atkinson and Aschmann [88]. They used the relative rate method with gas chromatographic analysis to determine rate constants for the reactions of chlorine atoms with benzene and toluene at room temperature and atmospheric pressure. Wallington et al. [95] reported rate constants for the reactions of chlorine atoms with benzene, toluene, *o*-xylene, *m*-xylene and *p*-xylene at ambient temperature and pressure, using the relative rate method with FTIR analysis. More recently Shi and Bernhard [100] also measured relative rate constants for the reaction of chlorine atoms with benzene, toluene, *o*-xylene, *m*-xylene, *p*-xylene, chlorobenzene and styrene at room temperature and atmospheric pressure. Markert and Pagsberg [101] determined the rate constant for the reaction of chlorine atoms with toluene using the absolute technique of pulse radiolysis combined with time-resolved ultraviolet spectroscopy.

In the course of their work on the benzylhydroperoxy radical, Nozière et al. [98] employed the relative rate method to determine rate constants for the reaction of chlorine atoms with benzene and toluene under ambient conditions of temperature and pressure. Bartels et al. [135] also determined the rate constant for the reaction of chlorine atoms with toluene using the relative rate technique during a study of the reactions of benzyl radicals with hydrogen atoms, oxygen atoms and molecular oxygen. Notario et al. [136] are currently studying the reactions of chlorine atoms with a series of aromatic compounds using the absolute technique of pulsed laser photolysis - resonance fluorescence. Their results to date are included in the discussion section.

While the rate constants reported for the reaction of chlorine atoms with toluene, *o*-xylene, *m*-xylene and *p*-xylene are all in good agreement there are discrepancies in the reported values for reaction of chlorine atoms with benzene. Nozière et al. [98] found that, in the presence of oxygen, the reaction is affected by the secondary formation of hydroxyl radicals. Berho et al. [99] studied this reaction in detail and found that the reactivity of benzene towards chlorine atoms is a function of the oxygen concentration and that no reaction occured in the absence of molecular oxygen. Shi and Bernhard [100] showed that, in the absence of molecular oxygen, the reaction is complicated by secondary radical reactions which may explain the discrepancies between previously reported values [88,95,98].

To date there has been little information regarding the mechanism for the reaction of chlorine atoms with aromatic compounds. The rate constants measured by Wallington et al. [95] for reaction of chlorine atoms with benzene, toluene and the xylenes led the authors to propose that, with the exception of benzene, the reactions proceed through a mechanism involving hydrogen atom abstraction from the substituent alkyl group(s). Markert and Pagsberg [101] measured the yield of benzyl radicals from the reaction of chlorine atoms with toluene and concluded that the reaction proceeds exclusively by H-atom abstraction from the methyl group.

Chlorine atoms may be present in significant amounts in the marine boundary layer (see Chapter 1) and hence could impact on the atmospheric chemistry of pollutants emitted in coastal zones. Aromatic compounds are emitted in large quantities in urban and industrial areas therefore it is important to understand the possible influence of chlorine atom chemistry. The main focus of the present study was to extend the database for reactions of chlorine atoms with aromatic compounds. The results of the study are compared with previously reported values and discussed in terms of structure-reactivity relationships, the mechanism for these reactions and atmospheric lifetimes.

2.2. EXPERIMENTAL

2.2.1. Relative Rate Studies

Materials

The materials used, their stated purities and their manufacturers are listed below.

Zero grade nitrogen and high purity air were obtained from Air Products Ltd. Nitrogen, air and hydrogen for the gas chromatograph and high purity oxygen were obtained from BOC Ltd.

Cyclohexane (99.5%), benzene (99%), toluene (99.5%), toluene-d_8 (100% atom D), o-xylene (98%), o-xylene-d_{10} (99+ atom % D), m-xylene (99+ %), p-xylene (99+ %), p-xylene-d_{10} (99+ %), p-xylene-d_6 (99+ %), 1,3,5-trimethylbenzene (98%), 1,2,4,5-tetramethylbenzene (98 %) o-ethyltoluene (99%), m-ethyltoluene (99%), p-ethyltoluene (99%), ethylbenzene (99%), n-propylbenzene (98%), n-butylbenzene (99+ %), 2-fluorotoluene (99+ %), 3-fluorotoluene (99%), 4-fluorotoluene (97%), 2-chlorotoluene (99+ %), chlorine (99.5+ %) and methane (99.0+ %) were obtained from Aldrich Chemical Company Ltd.

Apparatus

The experimental arrangement is shown in Figure 2.1. It consisted of a pyrex vacuum line combined with a 50dm^3 FEP collapsible Teflon reaction chamber. The chamber was surrounded by sixteen photolysis lamps (Thorn 40W White 3500) and housed in a commercial deep freeze cabinet.

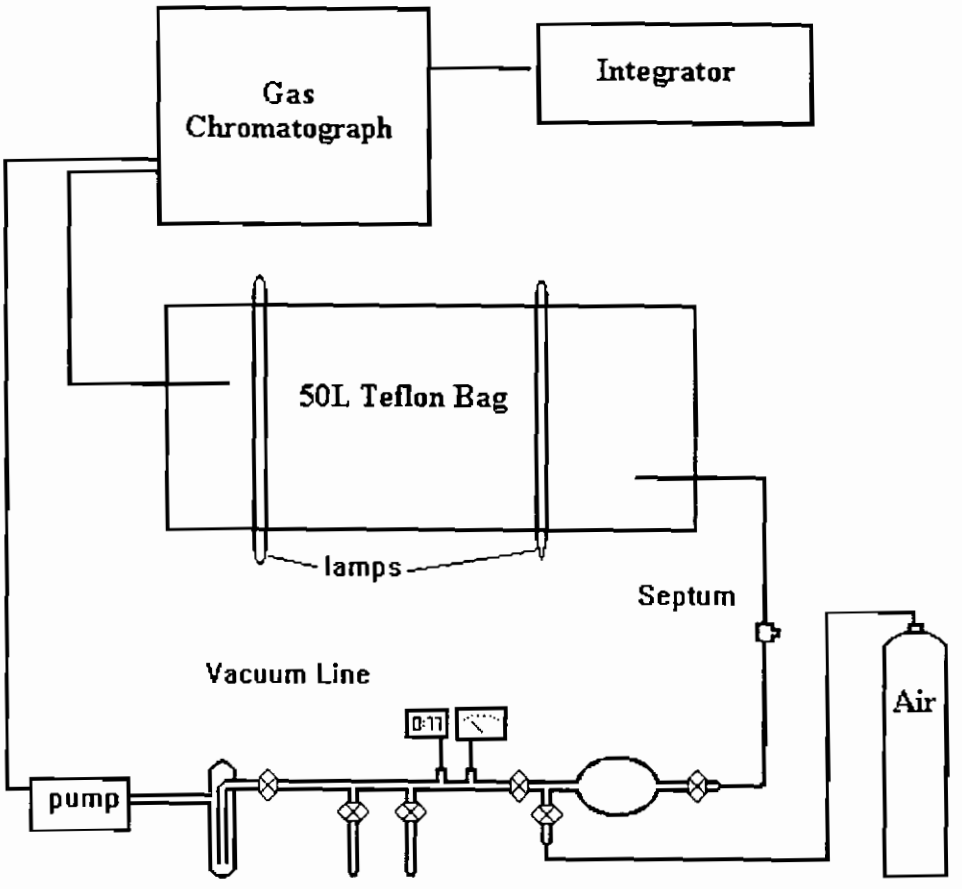

Figure 2.1. Schematic of Apparatus used in the Relative Rate Study

The vacuum was maintained by means of an Edwards direct drive rotary vane pump (model E2M2) in combination with a cryogenic trap. Taps were of the greaseless variety with Teflon O-rings obtained from J. Young Ltd. The vacuum was monitored using an Edwards pressure gauge (model PR-10K) connected to a readout unit (Edwards Pirani 10). Reactant pressures were measured using an Edwards Barocel pressure sensor (type 600AB, 0-10 Torr) in conjunction with a digital readout unit (Chell MK 7576). The reaction temperature was maintained at 298 ± 2 K using a combination of hot air blowers and fans and monitored by a thermocouple placed in the centre of the chamber.

Procedure

The diluent gas cylinder of zero-grade air, nitrogen or oxygen was connected to a 131 cm^3 mixing bulb via a digital flowmeter (Aalborg GFM17) using 1/4" O.D. Teflon tubing and the mixing bulb was connected to the 50dm^3 FEP Teflon bag using 1/8" O.D. Teflon tubing, thus allowing the controlled passage of diluent gas into the bag. The reaction chamber was cleaned before each experiment by flushing it several times with diluent gas. A gas chromatographic analysis of the emptying diluent gas was performed to ensure that no contaminants remained from previous experiments. Prior to addition of reactant, the bag was filled to approximately half its volume with diluent gas to minimise wall loss. The vacuum line and mixing bulb were then evacuated to $<10^{-3}$ Torr pressure. Each of the reactants (molecular chlorine, aromatic substrate and reference organic) was degassed at 77K prior to use. The aromatic substrate vapour was

shared from a storage vessel into the vacuum line and mixing bulb to a desired pressure, typically 0.3 - 6 Torr. A reactant pressure of 1 Torr in the 131 cm^3 mixing bulb corresponded to a mixing ratio of 3.4 ppm (1 ppm = 2.46 x 10^{13} molecules cm^{-3} at 298 K and 760 Torr). The mixing bulb was then isolated from the remainder of the vacuum line and the reactant flushed into the reaction chamber with diluent gas. The remainder of the reactant in the vacuum line was frozen back into its storage vessel using liquid nitrogen. This procedure was repeated for the reference organic and molecular chlorine and the bag subsequently filled to capacity with diluent gas. The reactants were allowed to mix in the dark for at least 30 minutes prior to photolysis. Uniform mixing was confirmed by gas chromatographic analysis of the reaction mixture.

Analysis

The reaction mixture was irradiated for two minute periods between which analysis of the reactants was carried out by gas chromatography (Ai Cambridge model GC94 series) fitted with a flame ionization detector. On-column injection of gas samples was carried out using a 2 cm^3 injection loop attached to a 6-port Valco gas sampling valve connected in series with the GC carrier gas flow circuit. Samples of the reaction mixture were drawn through the injection loop using the rotary vane pump. Chromatograms were recorded and stored on a computing integrator (Spectra-Physics Data Jet). Concentrations of aromatic substrate and reference organic were determined by measuring peak heights and peak areas. Table 2.2. shows the reference organics and analytical conditions used for each aromatic substrate.

Table 2.2. Reference organics and gas chromatographic conditions used for each aromatic compound studied in this work.

Aromatic Substrate	Reference Organic	Type	Column Length / m	Internal Diameter / mm	Column Temp / °C	Detector Temp / °C	N_2 Flow / ml min^{-1}
benzene	methane	DB-5	30	0.53	28	85	10
toluene	cyclohexane	DB-5	30	0.53	60	80	10
toluene-d_8	cyclohexane	DB-5	30	0.53	40	85	10
o-xylene	cyclohexane	DB-1	30	0.53	60	100	10
o-xylene-d_{10}	cyclohexane	DB-5	30	0.53	40	100	10
m-xylene	cyclohexane	DB-5	30	0.53	30→55	90	10
p-xylene	cyclohexane	DB-5	30	0.53	65	85	10
p-xylene-d_{10}	cyclohexane	DB-1	30	0.53	48	120	10
p-xylene-d_6	cyclohexane	DB-1	30	0.53	46	120	10
1,3,5-trimethylbenzene	cyclohexane	DB-5	30	0.53	65	85	10
1,2,4,5-tetra methylbenzene	cyclohexane	DB-1	30	0.53	100	160	10
o-ethyltoluene	cyclohexane	DB-1	30	0.53	100	130	10
m-ethyltoluene	cyclohexane	DB-1	30	0.53	95	130	10
p-ethyltoluene	cyclohexane	DB-1	30	0.53	100	130	10
ethylbenzene	cyclohexane	DB-5	30	0.53	30→60	85	10
n-propylbenzene	cyclohexane	DB-1	30	0.53	65	90	10
n-butylbenzene	cyclohexane	DB-1	30	0.53	90	140	10
2-fluorotoluene	cyclohexane	DB-1	30	0.53	90	120	10
3-fluorotoluene	cyclohexane	DB-1	30	0.53	40	120	10
4-fluorotoluene	cyclohexane	DB-1	30	0.53	40	120	10
2-chlorotoluene	cyclohexane	DB-1	30	0.53	90	120	10

2.2.2. Absolute Rate Studies using Pulsed Laser Photolysis - Resonance Fluorescence

Materials

Helium carrier gas (UHP certified to >99.9995%, Alphagaz) was passed from tank to cell through a liquid nitrogen trap. Chlorine (99.8%, UCAR) was degassed several times at 77K before use. Oxygen was certified to >99.995 % (Alphagaz). The aromatics 2-fluorotoluene (99+%, Aldrich), 3-fluorotoluene (99%, Aldrich) and 4-fluorotoluene (>99%, Aldrich) were degassed a number of times at 77K before use.

Apparatus

A schematic diagram of the pulsed laser photolysis-resonance fluorescence (PLP-RF) apparatus used in this study is shown in Figure 2.2. A Nd:YAG laser was used to generate chlorine atoms in the system by dissociation of the molecular chlorine precursor. The concentration of the chlorine atoms was measured by resonance fluorescence using a chlorine atom resonance lamp.

The reaction cell was constructed of Pyrex and had an internal volume of about 200 cm^3. The pressure in the cell was regulated by means of calibrated mass flow meters (Tylan FC260 and FC2901) and monitored with a pressure gauge (Tylan CDLC-31). Evacuation was achieved by means of a rotary vacuum pump attached via an adjustable valve.

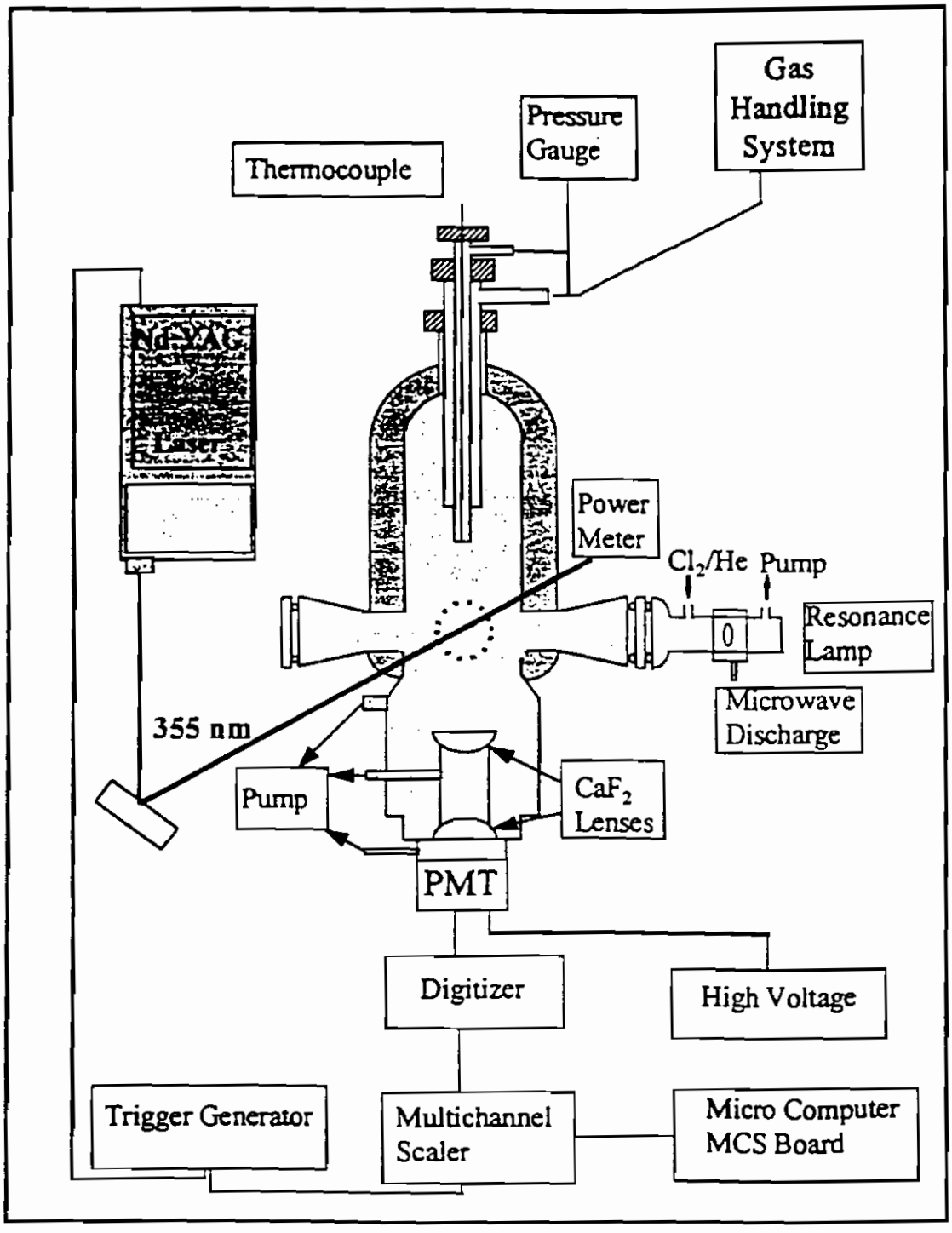

Figure 2.2. Schematic of Apparatus used in the PLP-RF Study of the Reaction of Chlorine Atoms with 2-, 3- and 4-Fluorotoluene

Cl atoms were produced by photolysing Cl_2 at 355 nm. The source of the 355 nm radiation was a pulsed, frequency tripled, Nd:YAG laser (Surelite II, from Continuum). The laser beam had a pulsewidth of 4-6 ns (full width at half maximum (fwhm)) and a linewidth of 0.002 nm. The chlorine atom concentration was monitored using a resonance fluorescence technique. Radiation at $\lambda \approx 135$ nm was used to excite resonance fluorescence from Cl atoms in the cell. The radiation was obtained from a microwave driven lamp, through which He containing ~ 0.3 % of Cl_2 flowed at P ~ 1.3 Torr. The lamp was situated perpendicular to the photolysis laser beam. A CaF_2 window was placed between the lamp and the cell. The resonance fluorescence was collected at 90° to both resonance lamp and photolysis laser beams by two CaF_2 lenses and imaged onto the photocathode of a solar blind photomultiplier tube (Hamamatsu R1459P). The regions between the two lenses and between the last lens and the photomultiplier were maintained under vacuum.

Procedure

In order to avoid accumulation of photolysis or reaction products, the experiments were carried out under slow flow conditions. The linear flow velocity through the cell was in the range 2 to 4 cm s^{-1} and the repetition rate of the photolysis laser was 10 Hz. Under these conditions, the gas mixture was flushed out from the interaction zone before the next laser pulse arrived. Reactant aromatics and Cl_2 were flowed from 10 litre bulbs containing dilute mixtures in helium. Concentrations of the different gases in the cell were calculated from measurements of the appropriate mass flow rates and the total

pressure. The mass flow meters (models FC 260 and FC 2901) and the pressure gauge (CDLC-31) were from Tylan General. Rate constants were measured at total pressures of 60 Torr and 15 Torr; in all cases the temperature was 298 ± 2 K. The main experimental error in the rate constant measurements comes from the uncertainty in the calculated concentration of the aromatics. This is estimated from the uncertainties in the flow rates and pressure readings which are estimated to be 2% and 1% respectively.

Signals were obtained using photon counting techniques in conjunction with multi-channel scaling. The fluorescence signal from the photomultiplier tube was processed by a digitizer (7803, Canberra) and sent to an EG&G multi-channel scaler (TP14P) to collect the time resolved signal. The multi-channel scaler was coupled to a microcomputer for imaging and analysis of the signals. Data acquisition was started prior to the photolysis pulse to obtain the background level of scattered light. A home made delay generator pre-triggered the acquisition before triggering the laser pulse. The background was subtracted from the post photolysis signal to obtain the temporal profile of the Cl atoms. The Cl temporal profiles following 5000 to 25000 laser pulses were coadded to enhance the signal to noise ratio. The detection limit for Cl atoms defined as $S/\sqrt{B} = 1$, (where S is the signal above the background, B) was around 8×10^9 atoms cm^{-3} for 1 second integration.

2.3. RESULTS

2.3.1. Relative Rate Method

The kinetic investigation was carried out using a relative rate technique which involves measuring the relative rates of disappearance of the aromatic substrate under investigation and a reference organic whose Cl atom rate constant is well known.

The aromatic substrate and reference organic react with atomic chlorine thus:

$$Cl\cdot + \text{aromatic substrate} \xrightarrow{k_s} \text{products} \qquad (2.9)$$

$$Cl\cdot + \text{reference organic} \xrightarrow{k_r} \text{products} \qquad (2.10)$$

Assuming that the loss process for the aromatic substrate and reference organic is solely via reactions (2.9) and (2.10),then

$$-d[\text{aromatic substrate}]/dt = k_s[Cl\cdot][\text{aromatic substrate}]$$

$$-d[\text{reference organic}]/dt = k_r[Cl\cdot][\text{reference organic}]$$

where k_s and k_r are the Cl atom rate constants for reactions (2.9) and (2.10) respectively.

Rearranging and integrating gives

$$\ln\left[\frac{[\text{aromatic substrate}]_{t_0}}{[\text{aromatic substrate}]_t}\right] = \frac{k_S}{k_r} \ln\left[\frac{[\text{reference organic}]_{t_0}}{[\text{reference organic}]_t}\right] \qquad \text{I}$$

where [aromatic substrate]$_{t0}$ and [reference organic]$_{t0}$, and [aromatic substrate]$_t$ and [reference organic]$_t$ are the concentrations of the aromatic substrate and reference organic at times t_0 and t respectively. Hence a plot of ln ([aromatic substrate]$_{t0}$/[aromatic substrate]$_t$) against ln ([reference organic]$_{t0}$/[reference organic]$_t$) should give a straight line of slope k_s/k_r with zero intercept. A knowledge of k_r from the literature allows k_s to be calculated from the slope.

When using the relative rate technique it is assumed that the only loss process for the aromatic substrate and reference organic is via reaction with chlorine atoms. To ensure that this condition was obeyed mixtures of molecular chlorine with the aromatic substrate and reference organic were allowed to stand in the dark over the timescale of the experiments. No significant loss of any of the reactants was observed. Mixtures of the aromatic substrate and reference organic were photolysed in the absence of molecular chlorine with no resultant loss of either being observed. Separate mixtures of chlorine with the aromatic substrate and reference organic were irradiated and analysed by gas chromatography to check for the formation of potentially interfering products in the gas chromatographic analysis.

The results obtained in this work were plotted in the form of equation I (Figures 2.3-2.12). Good linear plots with zero intercepts were obtained (with the exception of benzene) for all aromatic substrates.

Table 2.3. shows the rate constant ratios obtained in this work for the reaction of chlorine atoms with a series of aromatic compounds at 298 K and 1 atm. total pressure. The rate constants were placed on an absolute basis using:

$$k_r (Cl + CH_4) = 1.0 \times 10^{-13} \text{ cm}^3 \text{ molecule}^{-1} \text{ s}^{-1} \quad [130]$$

$$k_r (Cl + c\text{-}C_6H_{12}) = 3.5 \times 10^{-10} \text{ cm}^3 \text{ molecule}^{-1} \text{ s}^{-1} \quad [137]$$

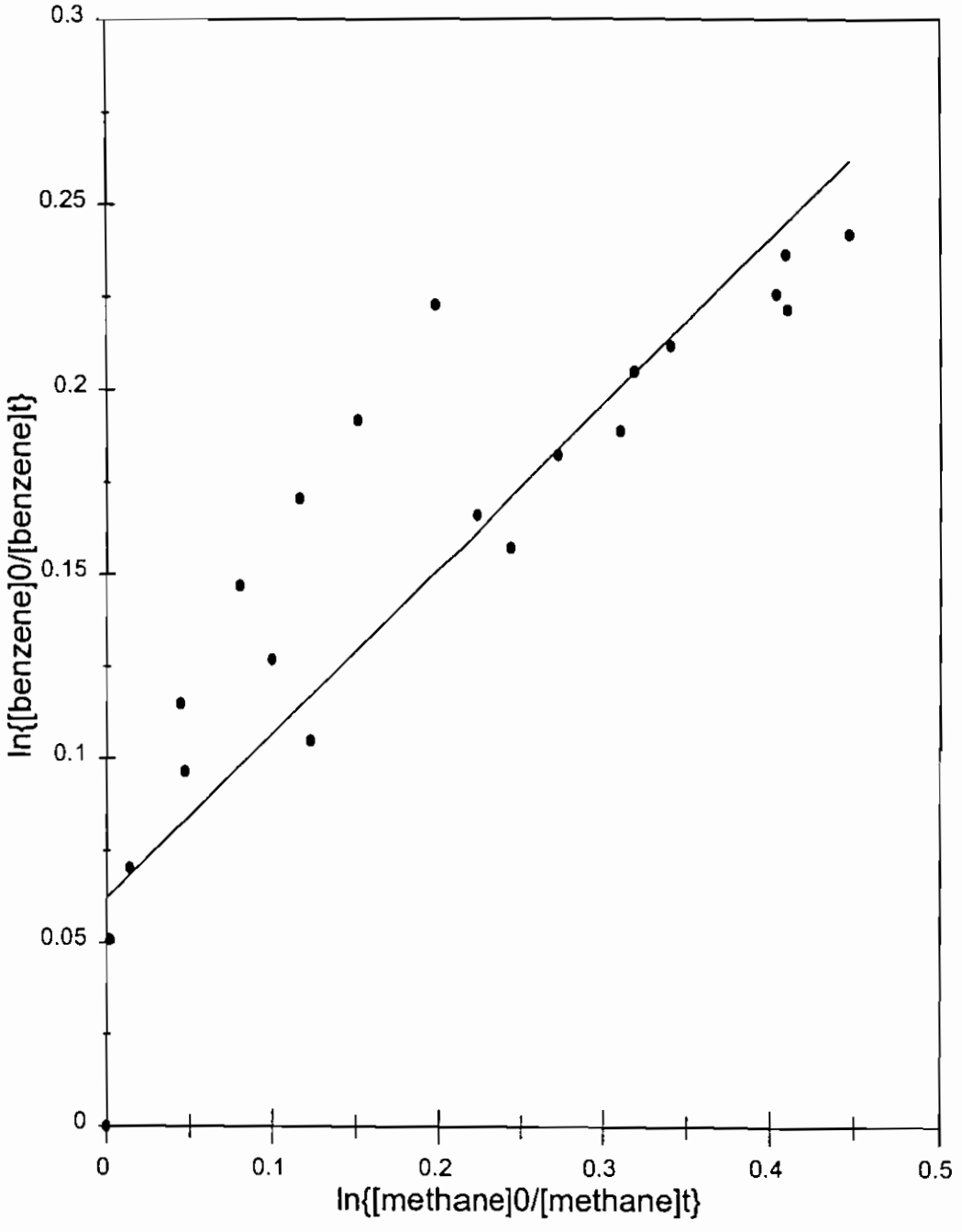

Figure 2.3. Plot in the form of equation I for the reaction of benzene with chlorine atoms at 298K and 1 atm. total pressure

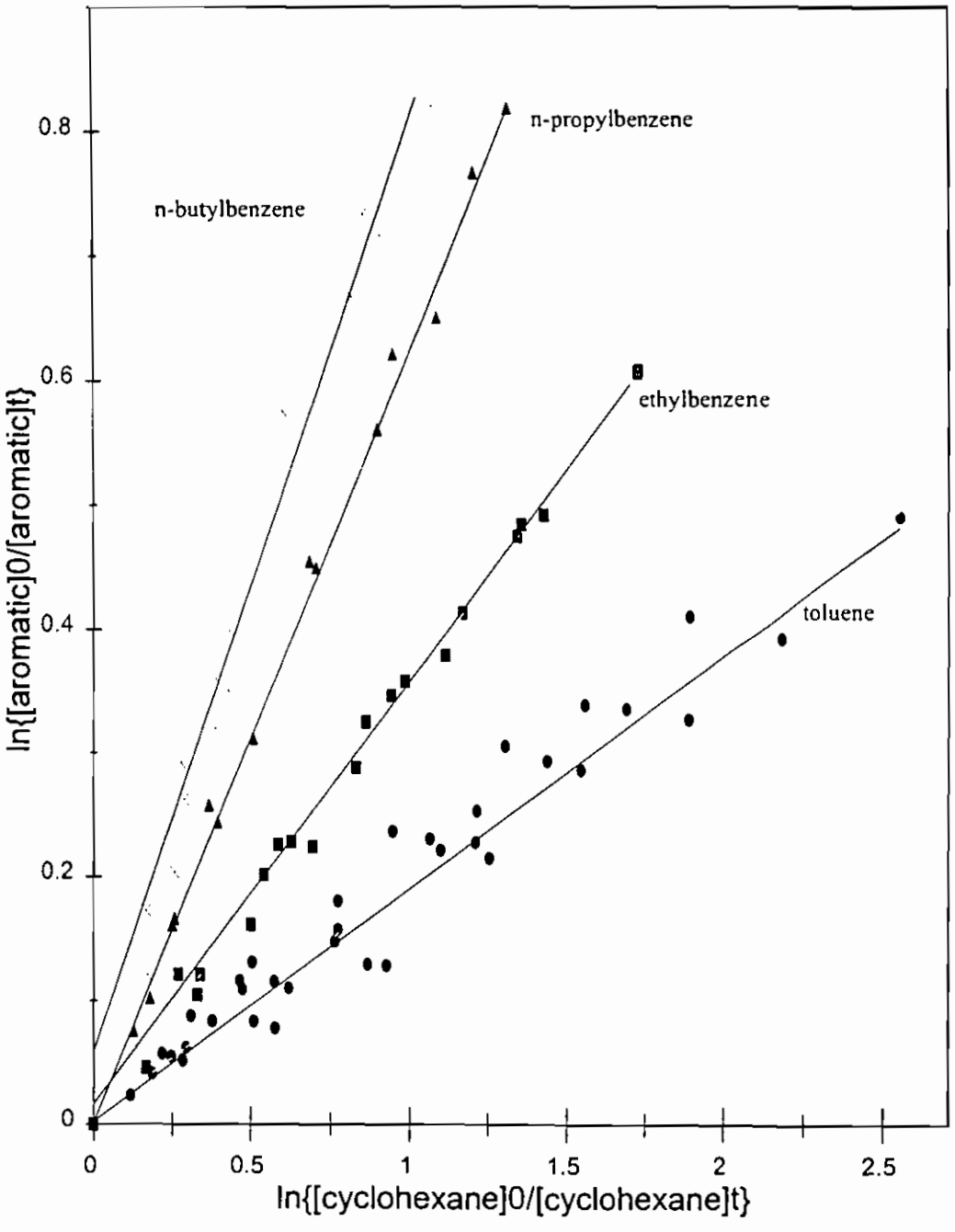

Figure 2.4. Plots in the form of equation I for the reaction of toluene, ethylbenzene, n-propylbenzene and n-butylbenzene with chlorine atoms at 298K and 1 atm. total pressure

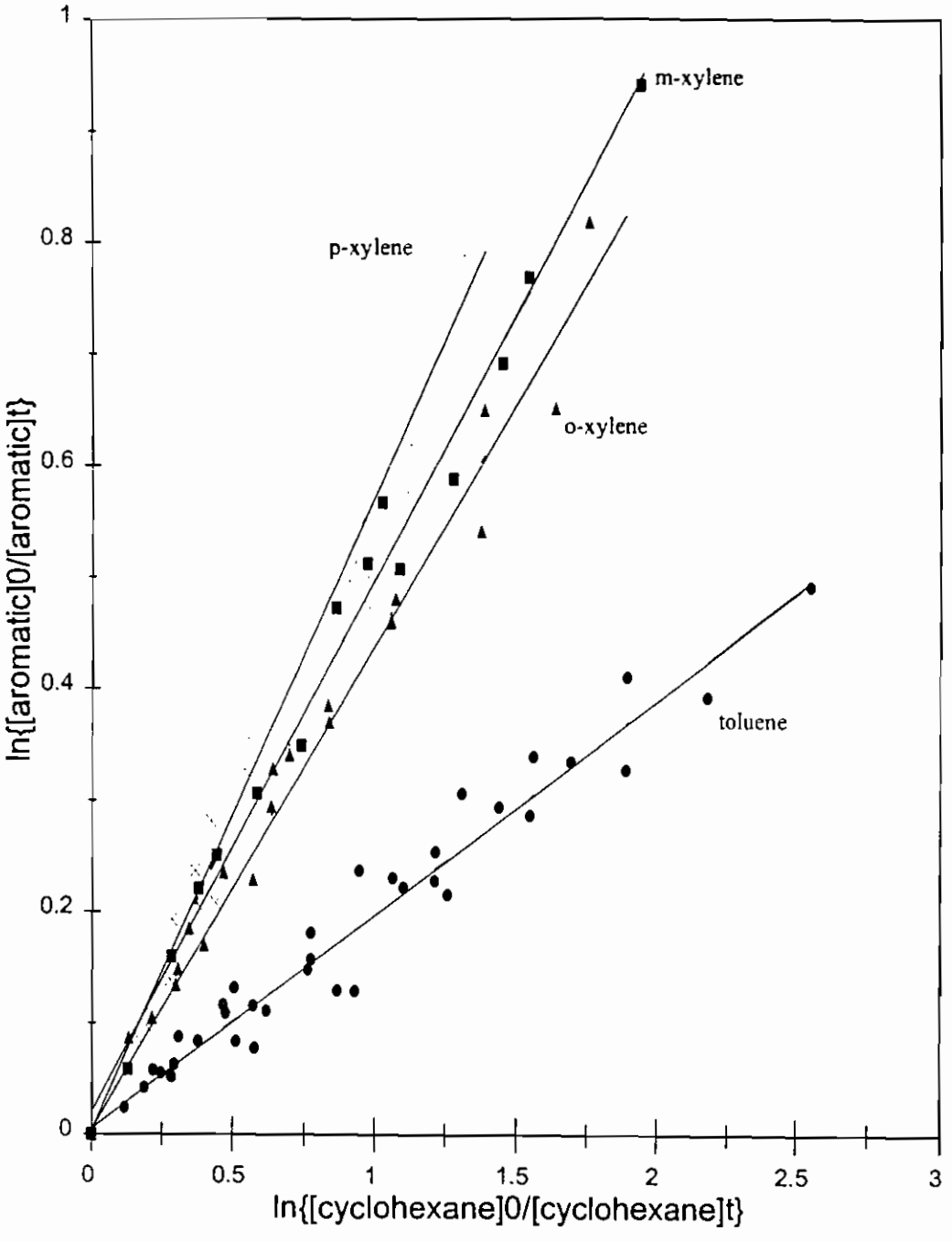

Figure 2.5. Plots in the form of equation I for the reaction of toluene, o-xylene, m-xylene and p-xylene with chlorine atoms at 298K and 1 atm. total pressure

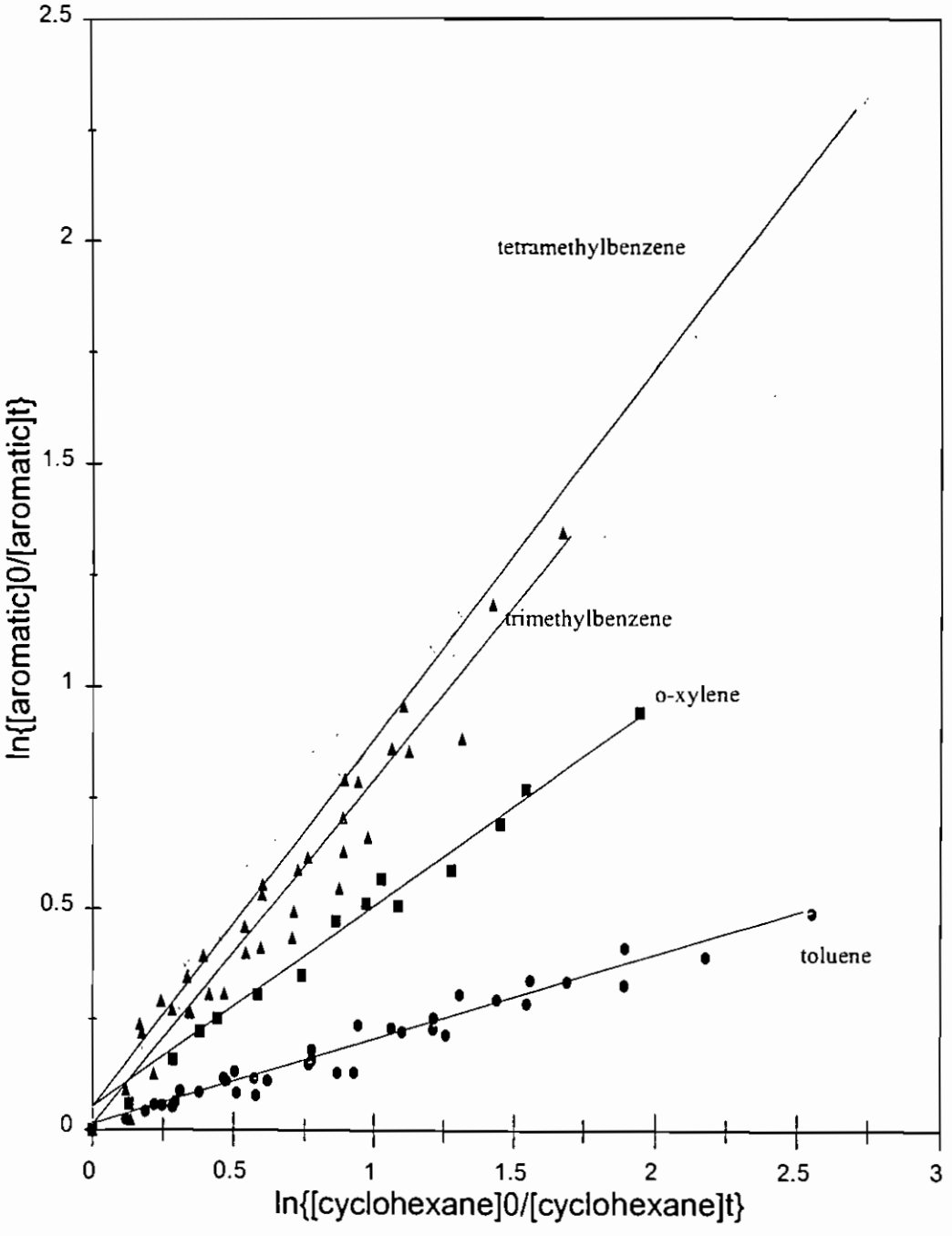

Figure 2.6. Plots in the form of equation I for the reaction of toluene, o-xylene, trimethylbenzene and tetramethylbenzene with chlorine atoms at 298K and 1 atm. total pressure

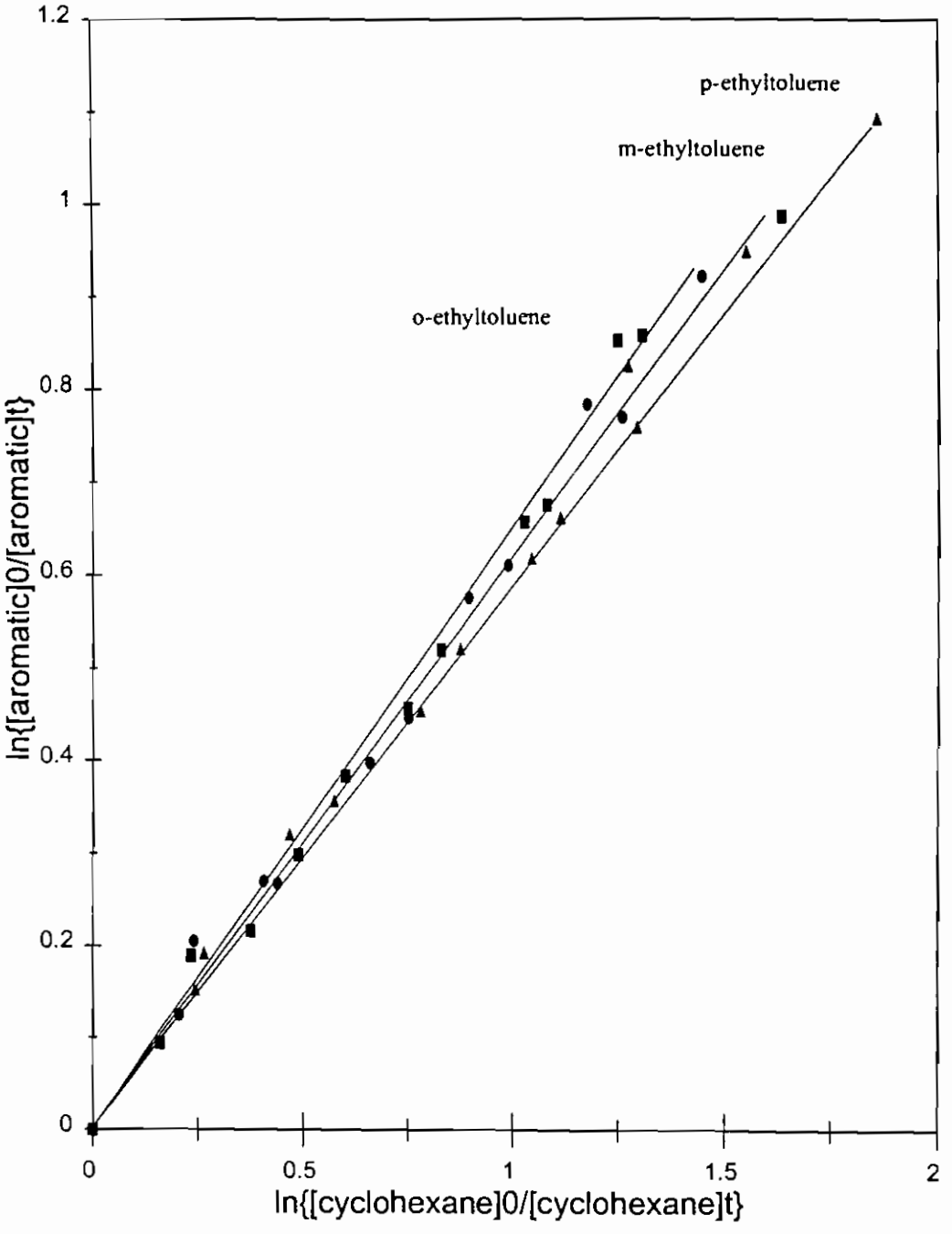

Figure 2.7. Plots in the form of equation I for the reaction of o-ethyltoluene, m-ethyltoluene and p-ethyltoluene with chlorine atoms at 298K and 1 atm. total pressure

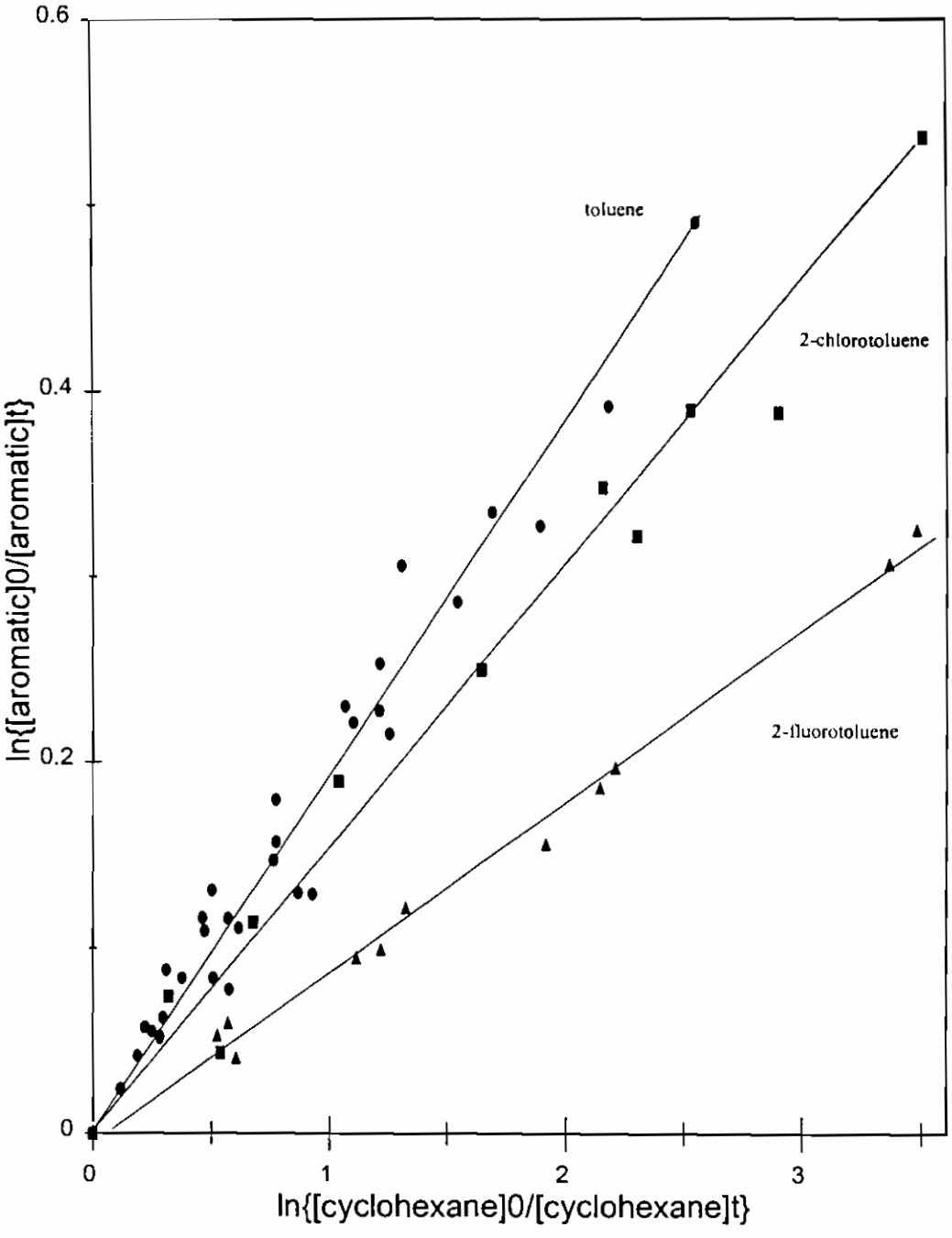

Figure 2.8. Plots in the form of equation I for the reaction of toluene, 2-chlorotoluene and 2-fluorotoluene with chlorine atoms at 298K and 1 atm. total pressure

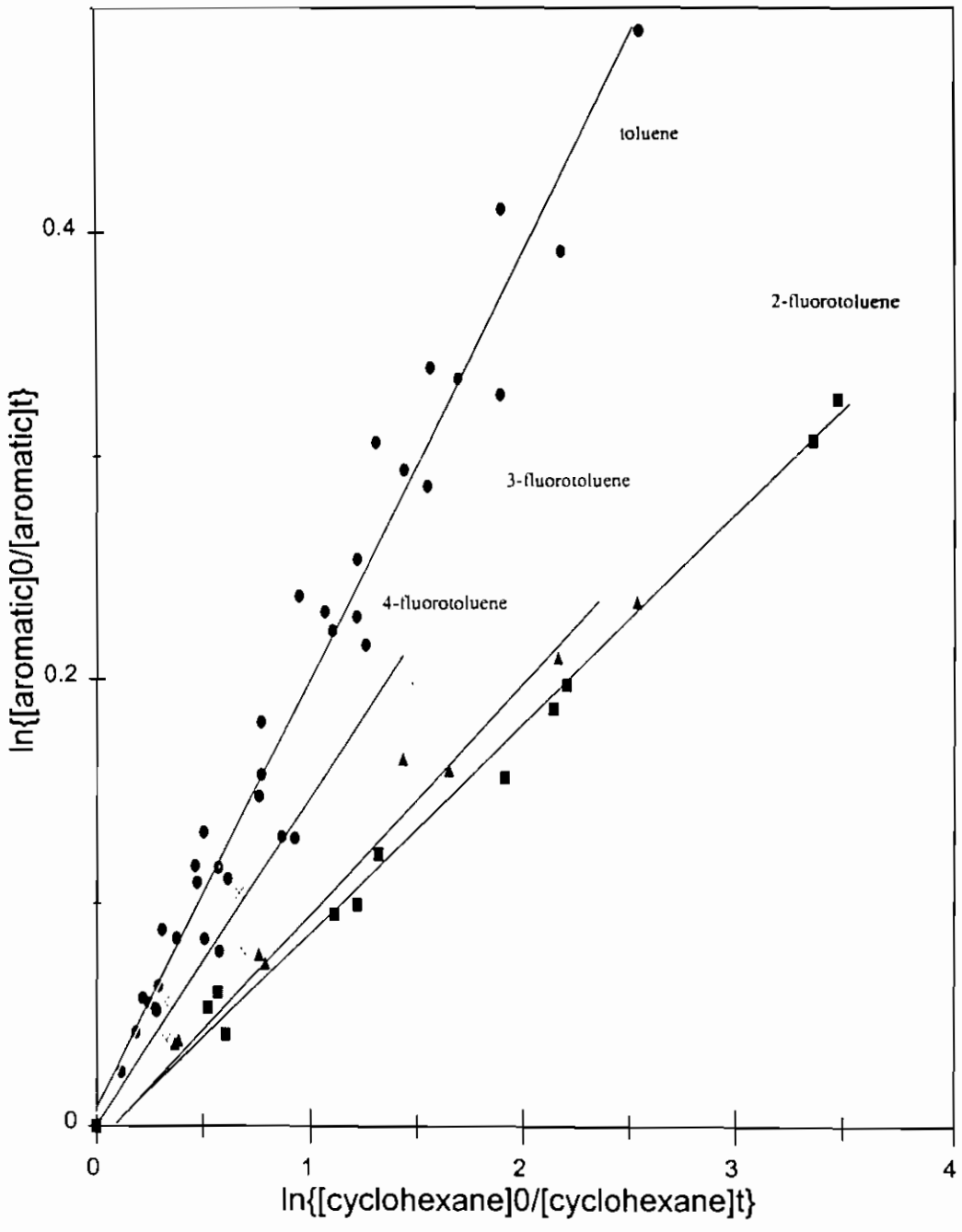

Figure 2.9. Plots in the form of equation I for the reaction of toluene, 2-fluorotoluene, 3-fluorotoluene and 4-fluorotoluene with chlorine atoms at 298K and 1 atm. total pressure

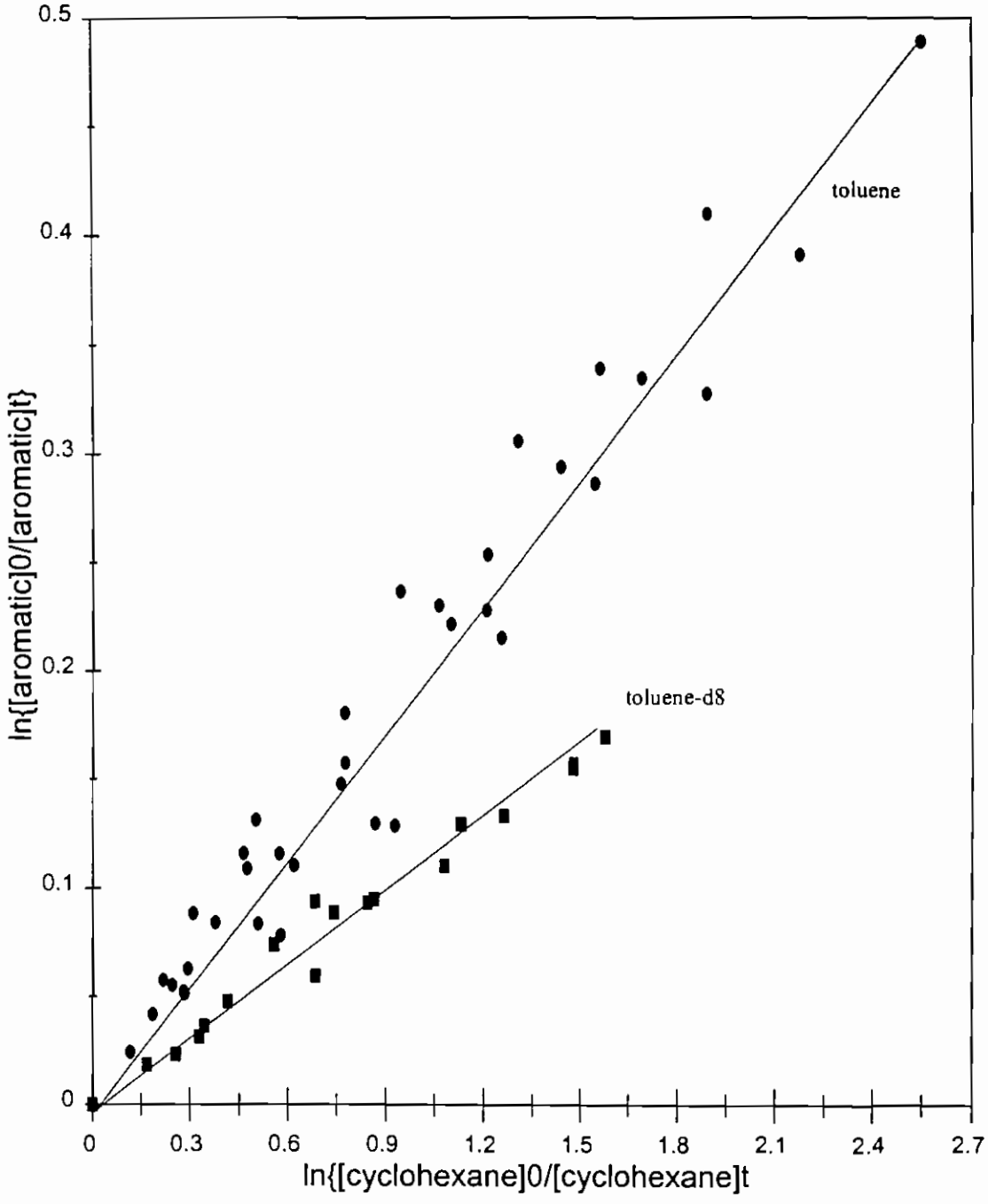

Figure 2.10. Plots in the form of equation I for the reaction of toluene and toluene-d_8 with chlorine atoms at 298K and 1 atm. total pressure

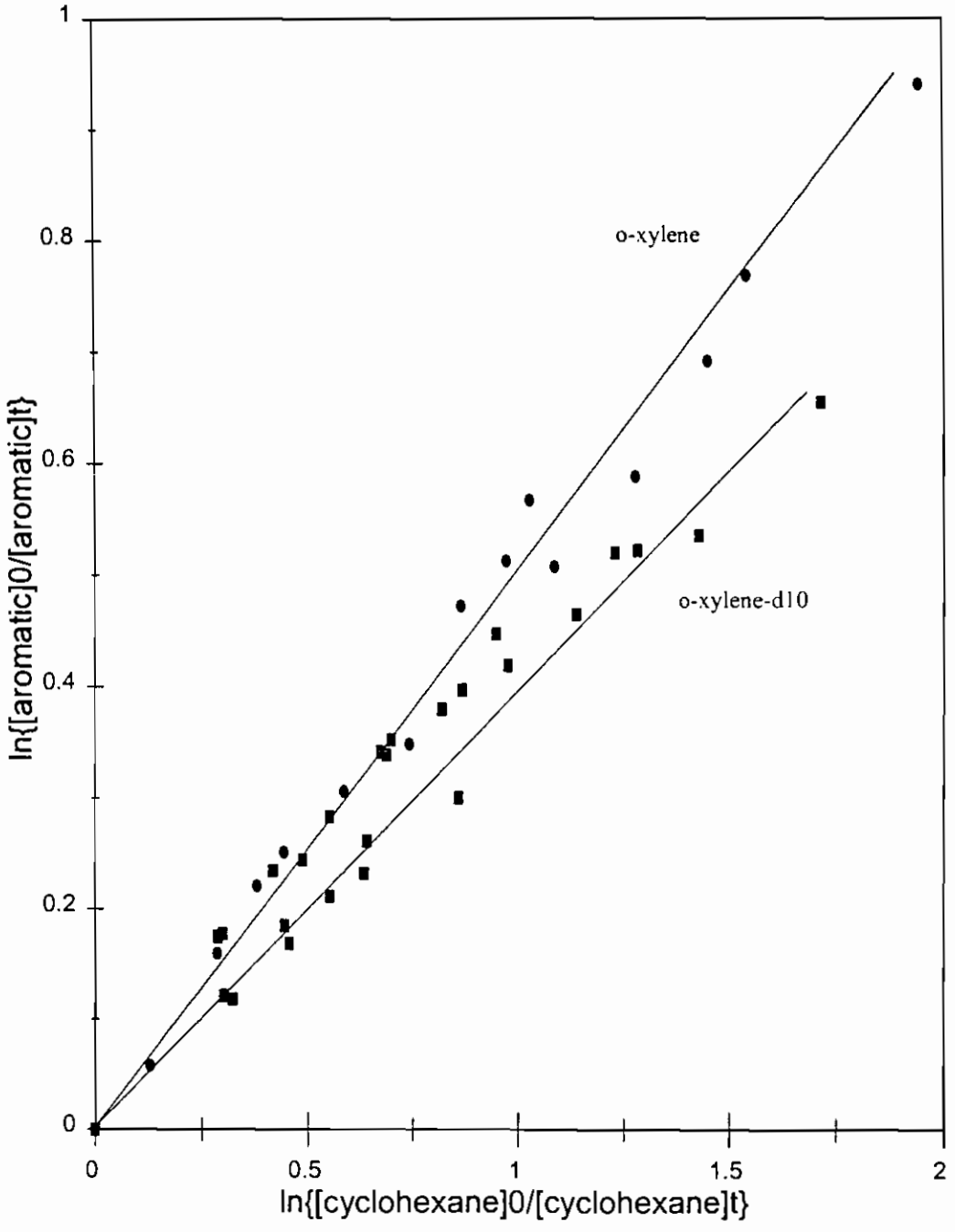

Figure 2.11. Plots in the form of equation I for the reaction of o-xylene and o-xylene-d_{10} with chlorine atoms at 298K and 1 atm. total pressure

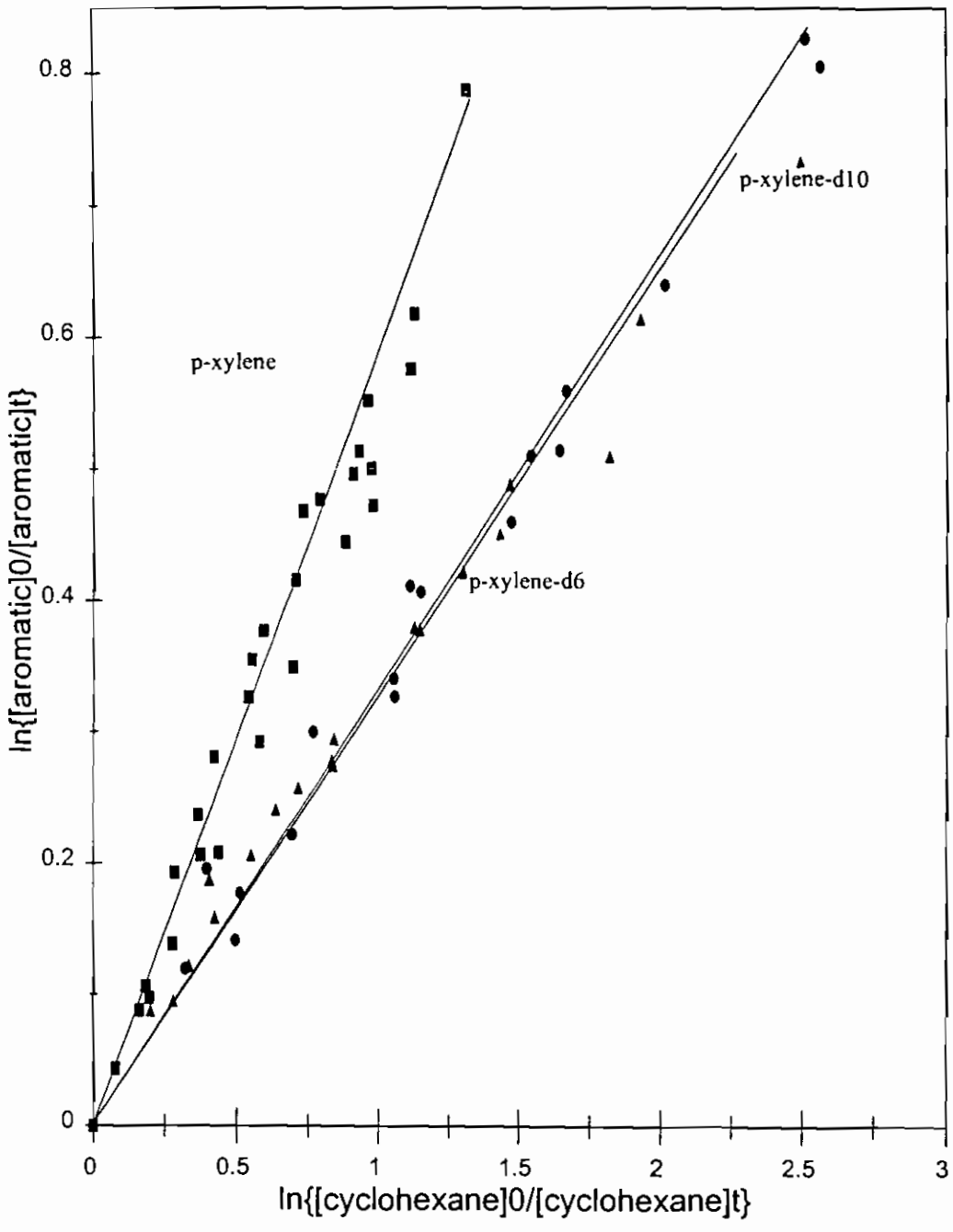

Figure 2.12. Plots in the form of equation I for the reaction of p-xylene, p-xylene-d_6, and p-xylene-d_{10} with chlorine atoms at 298K and 1 atm. total pressure

Table 2.3. Rate constant ratios, k_s/k_r, and rate constants, k_s, for the reaction of chlorine atoms with a series of aromatic compounds determined in this work at 298 ± 2 K and 1 atm. total pressure

Substrate	k_s/k_r [a]	$10^{11} \times k_s$ [b] cm^3 $molecule^{-1}$ s^{-1}
benzene	0.35 ± 0.12	<0.1
toluene	0.19 ± 0.12	6.70 ± 0.41
toluene-$\mathbf{d_8}$	0.11 ± 0.01	3.75 ± 0.24
o-xylene	0.48 ± 0.03	16.9 ± 0.8
o-xylene-$\mathbf{d_{10}}$	0.39 ± 0.03	13.7 ± 1.0
m-xylene	0.43 ± 0.02	15.0 ± 0.8
p-xylene	0.55 ± 0.03	19.1 ± 0.6
p-xylene-$\mathbf{d_{10}}$	0.29 ± 0.02	10.1 ± 0.6
p-xylene-$\mathbf{d_6}$	0.30 ± 0.02	10.4 ± 0.6
1,3,5-trimethylbenzene	0.77 ± 0.05	26.8 ± 1.8
1,2,4,5-tetramethylbenzene	0.82 ± 0.04	28.8 ± 1.5
o-ethyltoluene	0.62 ± 0.03	21.9 ± 1.0
m-ethyltoluene	0.63 ± 0.03	22.1 ± 1.1
p-ethyltoluene	0.59 ± 0.03	20.7 ± 0.8
ethylbenzene	0.35 ± 0.01	12.3 ± 0.3
n-propylbenzene	0.63 ± 0.02	21.9 ± 0.6
n-butylbenzene	0.79 ± 0.06	28.0 ± 1.8
2-fluorotoluene	0.10 ± 0.01	3.38 ± 0.36
3-fluorotoluene	0.10 ± 0.01	3.34 ± 0.26

Table 2.3. continued

4-fluorotoluene	0.14 ± 0.01	4.96 ± 0.45
2-chlorotoluene	0.12 ± 0.02	4.94 ± 0.79

a Errors quoted are two least-squares standard deviations of the slopes of the plots shown in Figures 2.3 - 2.12. Errors quoted do not include systematic error.

b Errors quoted do not include the error in the rate constant for reaction of chlorine atoms with the reference organic.

2.3.2. Absolute Method

For a reaction mixture containing Cl_2, the aromatic substrate (RH) in helium as diluent, and in the absence of secondary reactions, the temporal profile of chlorine atoms is governed by the following reactions:

$$Cl + RH \xrightarrow{k} \text{products} \qquad (2.11)$$

$$Cl \xrightarrow{k0} \text{loss by diffusion} \qquad (2.12)$$

Experiments were carried out under psuedo first order conditions with the concentration of the aromatic in large excess over the chlorine atom concentration. Typically, the concentration of Cl_2 was approx. 3×10^{13} molecules cm^{-3} giving an initial concentration of chlorine atoms, $[Cl]_0$, of around 5×10^{11} atoms cm^{-3}. The initial concentration of the aromatic substrate was 7-335 x 10^{12} molecules cm^{-3}. Under these conditions, the rate of disappearance of Cl atoms follows a simple exponential rate law:

$$[Cl]_t = [Cl]_0 \exp(-k't) \qquad \text{where } k' = k[RH] + k_0$$

where k' is the pseudo first order rate constant,

k is the bimolecular rate constant for the reaction of Cl with the aromatic substrate, and

[RH] is the aromatic concentration.

The first order decay rate of Cl in the absence of the aromatic, k_0, is the diffusion rate of Cl atoms out of the detection zone. Under the experimental conditions, k_0 was ~ 40 s^{-1} at P = 60 Torr and ~ 60 s^{-1} at P = 15 Torr.

The initial concentration of Cl used was around 3-5 x 10^{11} molecules cm^{-3} in order to get a sufficient signal to noise ratio. This concentration was obtained with a Cl_2 concentration of ca. 3 x 10^{13} molecules cm^{-3} and 15 to 30 mJ/pulse as photolysis fluence at 355 nm. The excess concentration ranges of the aromatics were (in 10^{12} molecules cm^{-3}): (28 - 335), (11 - 220), (7 - 110), for 2-fluorotoluene, 3-fluorotoluene and 4-fluorotoluene respectively.

Oxygen was added to the reaction mixture to avoid the regeneration of Cl via the reaction:

$$R + Cl_2 \rightarrow RCl + Cl \qquad (2.13)$$

where R refers to $C_6H_4FCH_2$

In the presence of oxygen the following reaction takes place:

$$R + O_2 \rightarrow \text{products} \qquad (2.14)$$

The O_2 concentration was limited by the efficient quenching of Cl atom fluorescence by O_2 and also by the absorption of the vacuum UV radiation from the fluorescence. The intensity of the fluoresence signal was reduced at least by a factor of 2 in the presence of $[O_2] = 10^{16}$ molecules cm^{-3}. It was found that the maximum O_2 pressure at which rate constants could be measured was 0.4 Torr. Some experiments were carried out with other aromatics in the absence of O_2 and the resulting rate constants were consistently lower than those measured with 0.4 Torr of O_2 although the difference was within the experimental errors.

The plots of $k' - k_0$ vs. the initial aromatic concentrations are shown in Figure 2.13. Bimolecular rate constants obtained at 15 Torr, 60 Torr and the overall value for reaction of Cl atoms with 2-fluorotoluene, 3-fluorotoluene and 4-fluorotoluene are shown in Table 2.4.

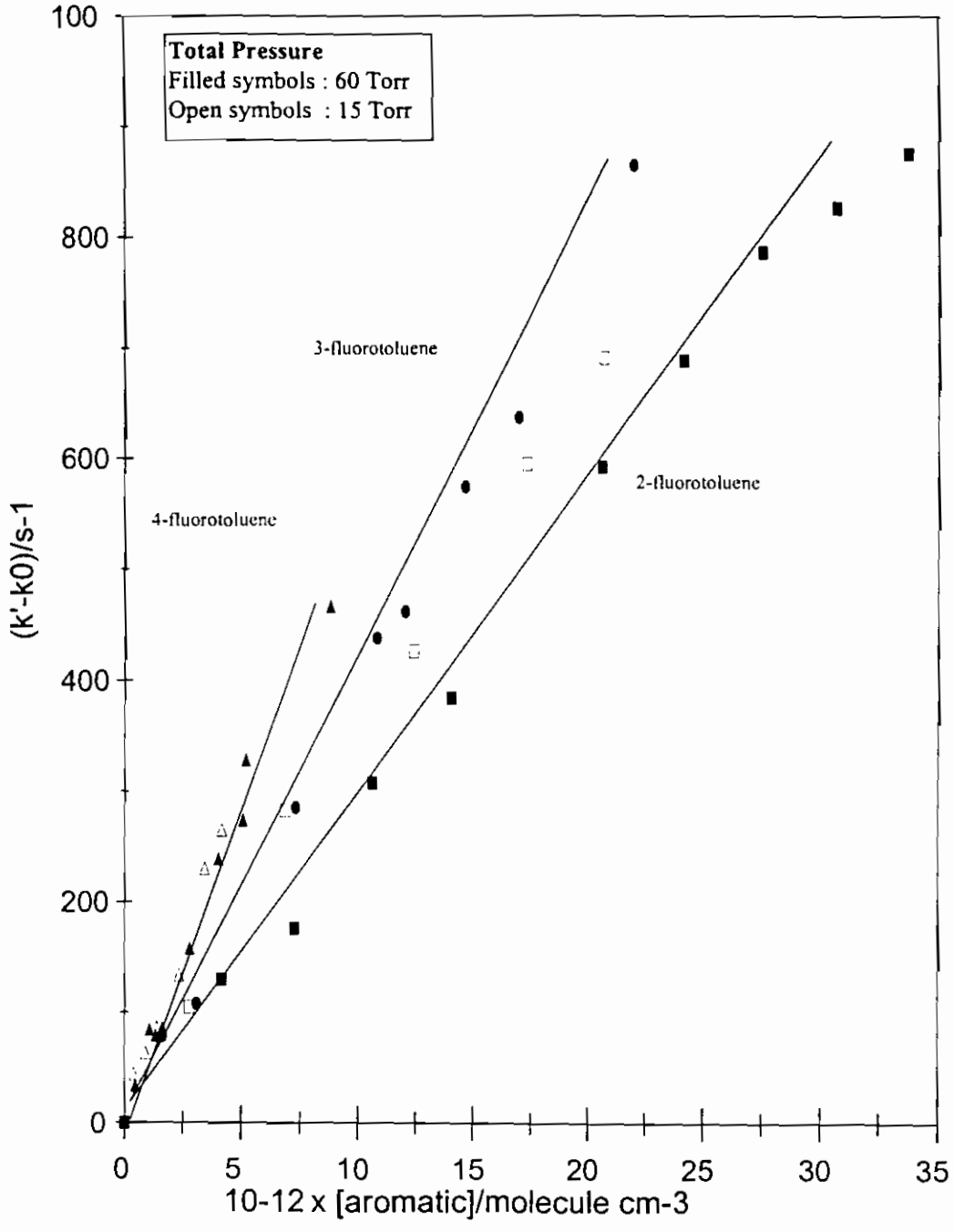

Figure 2.13. Plots of (k'- k_0) versus concentration of 2-fluorotoluene, 3-fluorotoluene and 4-fluorotoluene at 298 ± 2 K.

Table 2.4. Rate constants for the reaction of chlorine atoms with a series of aromatic compounds at 298 ± 2 K using the technique of pulsed laser photolysis-resonance fluorescence

Aromatic Substrate	[Aromatic] / molecules cm^{-3}	P = 15 Torr k[a] / cm^3 $molecule^{-1}$ s^{-1}	P = 60 Torr k / cm^3 $molecule^{-1}$ s^{-1}	Overall[b] k / cm^3 $molecule^{-1}$ s^{-1}
2-fluorotoluene	(28 - 335) x 10^{12}	3.43 ± 0.17 x 10^{-11}	2.75 ± 0.08 x 10^{-11}	2.87 ± 0.16 x 10^{-11}
3-fluorotoluene	(11 - 220) x 10^{12}	4.45 ± 0.24 x 10^{-11}	3.90 ± 0.08 x 10^{-11}	4.00 ± 0.15 x 10^{-11}
4-fluorotoluene	(7 - 110) x 10^{12}	5.74 ± 0.42 x 10^{-11}	5.59 ± 0.35 x 10^{-11}	5.67 ± 0.26 x 10^{-11}

a Errors quoted are two least-squares standard deviations of the slopes of the plots shown in Figure 2.13. Errors quoted do not include systematic error which is likely to be 5-10 %.

b The overall rate constant was calculated from the slope of a plot of all the values obtained at 15 Torr total pressure and 60 Torr total pressure

2.4. DISCUSSION

Room temperature rate constants obtained in this study for the reaction of chlorine atoms with a series of aromatic compounds are shown in Table 2.5, together with the available literature data. There is good agreement between the relative and absolute rate constants obtained in this work for 2-, 3- and 4-fluorotoluene. The pulsed laser photolysis - resonance fluorescence technique employed in this work was also used by Notario et al. [136] to determine absolute rate constants for reaction of chlorine atoms with a series of aromatic hydrocarbons. The rate constants determined during that study, which are also included in Table 2.5, are in very good agreement with the relative rate constants obtained in this work. This agreement lends confidence to the accuracy of the rate data obtained by the relative rate method.

Previously reported rate constants for the reaction of chlorine atoms with benzene show poor agreement. The value obtained by Atkinson and Aschmann [88] is several orders of magnitudes greater than that obtained by Wallington et al. [95], Nozière et al. [98], Berho et al. [99] and Shi et al. [100]. Nozière et al. [98] carried out relative rate studies on the reaction of chlorine atoms with benzene, using methane as the reference compound. They found that the results varied with different diluent gases. When air was used the relative rate plots were curved whereas in nitrogen there was no observable benzene loss but all the methane was consumed. The authors attributed this difference to the secondary formation of OH radicals from the reaction of chlorine with methane in

the presence of O_2. The following mechanism can be used to explain the production of OH [138]:

CH_4	+	Cl	→	CH_3	+	HCl	(2.15)
CH_3	+	O_2	→	CH_3O_2			(2.16)
CH_3O_2	+	CH_3O_2	→	2 CH_3O	+	O_2	(2.17)
CH_3O	+	O_2	→	HCHO	+	HO_2	(2.18)
CH_3O_2	+	HO_2	→	CH_3OOH	+	O_2	(2.19)
CH_3OOH	+	Cl	→	CH_2OOH	+	HCl	(2.20)
		CH_2OOH	→	HCHO	+	OH	(2.21)

Hydroxyl radicals react 170 times more rapidly with benzene than with methane [139] and thus cause an enhancement of the benzene decay. The authors proposed that the unusually high value of $k(Cl + C_6H_6) = 1.5 \pm 0.9 \times 10^{-12}$ cm^3 molecule^{-1} s^{-1} reported by Atkinson and Aschmann [88] could be rationalised in terms of the above mechanism.

More recently Berho et al. [99] also investigated the effect of molecular oxygen on the reaction of chlorine atoms with benzene. Using a flash photolysis - UV absorption technique the authors observed no reaction between chlorine atoms and benzene in the absence of oxygen. The relative rate method was used to determine a value for $k(Cl + C_6H_6) = 8.9 \pm 1.6 \times 10^{-14}$ cm^3 molecule^{-1} s^{-1} in the presence of oxygen at 298K and 1 atm. total pressure.

Table 2.5. Rate constants for the reaction of chlorine atoms with aromatic compounds at 298 K

Substrate	[a] $10^{11} \times k_{Cl}$ cm^3 $molecule^{-1}s^{-1}$	Literature Reference
benzene 	1.5 ± 0.9	Atkinson et al. [88]
	<0.4	Wallington et al. [95]
	< 0.00005	Nozière et al. [98]
	0.0089 ± 0.0016	Berho et al. [99]
	0.00013 ± 0.00003	Shi et al. [100]
	<0.1	**This Work**
toluene 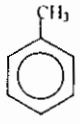	5.89 ± 0.36	Atkinson et al. [88]
	5.59 ± 0.28	Wallington et al. [95]
	5.81 ± 1.81	Bartels et al. [135]
	5.65 ± 0.60 [b]	Markert et al. [101]
	6.1 ± 0.2	Nozière et al. [98]
	5.9 ± 0.5	Shi et al. [100]
	5.98 ± 0.08 [c]	Notario et al. [136]
	6.70 ± 0.41	**This Work**
toluene-d_8 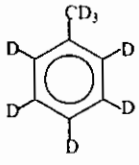	3.75 ± 0.24	**This Work**
o-xylene 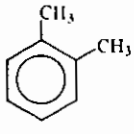	12.0 ± 0.9	Wallington et al. [95]
	15 ± 1	Shi et al. [100]
	16.2 ± 0.8 [c]	Notario et al. [136]
	16.9 ± 0.8	**This Work**

Table 2.5 Continued...

o-xylene-d_{10} 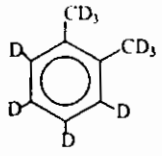	13.7 ± 1.0	**This Work**
m-xylene 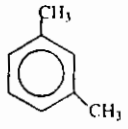	12.0 ± 1.4 14 ± 1 12.7 ± 0.7 c 15.0 ± 0.8	Wallington et al. [95] Shi et al. [100] Notario et al. [136] **This Work**
p-xylene 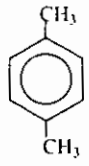	13.3 ± 0.8 15 ± 1 15.3 ± 0.8 c 19.1 ± 0.6	Wallington et al. [95] Shi et al. [100] Notario et al. [136] **This Work**
p-xylene-d_{10} 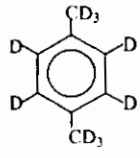	10.1 ± 0.6	**This Work**
p-xylene-d_6 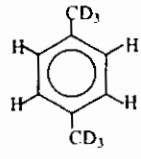	10.4 ± 0.6	**This Work**

Table 2.5 Continued...

1,3,5-trimethylbenzene 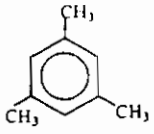	17.8 ± 0.3 c 26.8 ± 1.8	Notario et al. [136] **This Work**
1,2,4,5-tetramethylbenzene 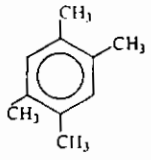	28.8 ± 1.5	**This Work**
o-ethyltoluene 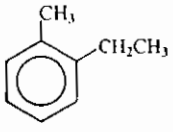	21.6 ± 0.7 c 21.9 ± 1.0	Notario et al. [136] **This Work**
m-ethyltoluene 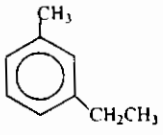	18.8 ± 0.4 c 22.1 ± 1.1	Notario et al. [136] **This Work**
p-ethyltoluene 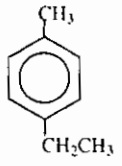	19.0 ± 0.8 c 20.7 ± 0.8	Notario et al. [136] **This Work**

Table 2.5 Continued...

ethylbenzene 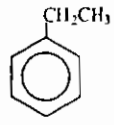	13.4 ± 0.6 [c] 12.3 ± 0.3	Notario et al. [136] **This Work**
n-propylbenzene 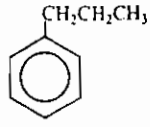	17.3 ± 0.6 [c] 21.9 ± 0.6	Notario et al. [136] **This Work**
n-butylbenzene 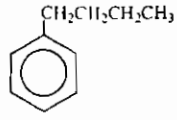	20.9 ± 0.7 [c] 28.0 ± 1.8	Notario et al. [136] **This Work**
2-fluorotoluene 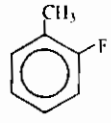	2.87 ± 0.16 [c] 3.38 ± 0.36	**This Work** **This Work**
3-fluorotoluene 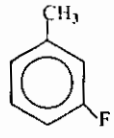	4.00 ± 0.15 [c] 3.34 ± 0.26	**This Work** **This Work**

Table 2.5 Continued...

4-fluorotoluene 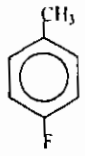	5.67 ± 0.26 [c] 4.96 ± 0.45	**This Work** **This Work**
2-chlorotoluene 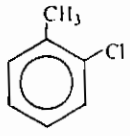	4.94 ± 0.79	**This Work**

a determined from relative rate measurements.
b determined using the absolute technique of pulse radiolysis combined with time-resolved ultraviolet spectroscopy.
c determined using the absolute technique of pulsed laser photolysis - resonance fluorescence at 15 Torr and 60 Torr total pressure.

Shi and Bernhard [100] studied the reaction of benzene with chlorine atoms using the relative rate technique with FTIR analysis. Experiments were carried out using either CHF_2Cl or CF_3CH_2F as the reference compound. The authors found that benzene was regenerated when using N_2 as the diluent gas via the following reactions:

$$Cl + C_6H_6 \rightarrow C_6H_5 + HCl \qquad (2.22)$$

$$C_6H_5 + CHF_2Cl \rightarrow C_6H_6 + CF_2Cl \qquad (2.23)$$

In air the C_6H_5 radical reacts rapidly with O_2 thus preventing the occurrence of reaction 2.23. A room temperature value of $k(Cl + C_6H_6) = 1.3 \pm 0.3 \times 10^{-15}$ cm^3 $molecule^{-1}$ s^{-1} was reported in 1 atm. of air using CHF_2Cl as the reference compound.

When CF_3CH_2F was used as the reference compound the rate constant ratio was dependent on the initial concentration of CF_3CH_2F. This was attributed to the formation of the CF_3O radical from the chlorine atom initiated oxidation of CF_3CH_2F and its subsequent reaction with both benzene and CF_3CH_2F:

$$CF_3O + C_6H_6 \rightarrow \text{Products} \qquad (2.24)$$

$$CF_3O + CF_3CH_2F \rightarrow CF_3OH + CF_3CHF \qquad (2.25)$$

In the course of the present study rate constants for reaction of chlorine atoms with benzene were measured in both air and nitrogen. The values obtained agreed within the experimental uncertainties. However, it is very likely that the nitrogen diluent contained some oxygen due to diffusion through the teflon bag. The room temperature rate constant obtained in this work provides an upper limit of 1×10^{-12} cm^3 molecule^{-1} s^{-1}, in broad agreement with Wallington et al. [95], Nozière et al. [94], Berho et al. [99] and Shi & Bernhard [100].

There are two possible pathways for reaction of chlorine atoms with benzene: abstraction of a hydrogen atom or addition of the chlorine atom to the aromatic ring:

$$C_6H_6 + Cl \rightarrow C_6H_5 + HCl \qquad (2.26)$$

$$C_6H_6 + Cl \leftrightarrow [C_6H_6Cl]^* \rightarrow \text{Products} \qquad (2.27)$$

where $[C_6H_6Cl]^*$ is the unstable intermediate that can either decompose back to the original reactants or further react to form products.

Shi and Bernhard [100] carried out product studies on the reaction of chlorine atoms with benzene in air diluent at 298K and 740 Torr total pressure using FTIR spectroscopy. They proposed that if reaction 2.27 occured to a significant extent C_6H_5Cl would be formed in the presence of O_2:

$$[C_6H_6Cl]^* + O_2 \rightarrow C_6H_5Cl + HO_2 \quad (2.28)$$

C_6H_5Cl was not observed suggesting that reaction 2.28 is not a significant reaction channel. The authors also studied the pressure dependence of this reaction in air between 10 and 740 Torr total pressure. No statistically significant pressure dependence was observed again suggesting that the addition channel is unimportant. The investigators concluded that H-atom abstraction is the dominant pathway for reaction of chlorine atoms with benzene.

The room temperature rate constant for reaction of chlorine atoms with toluene obtained in this study is in good agreement with previously reported values using both absolute [101,136] and relative rate techniques [88,95,98,100,135] while the rate constant data for reaction of chlorine atoms with *ortho*-, *meta*- and *para*-xylene are in good agreement with the values obtained by Wallington et al. [95], Shi and Bernhard [100] and Notario et al. [136].

This study represents the first reported rate data for reaction of chlorine atoms with toluene-d_8, *o*-xylene-d_{10}, *p*-xylene-d_{10}, *p*-xylene-d_6, 1,3,5-trimethylbenzene, 1,2,4,5-tetramethylbenzene, *o*-ethyltoluene, *m*-ethyltoluene, *p*-ethyltoluene, ethylbenzene, n-propylbenzene, n-butylbenzene, 2-fluorotoluene, 3-fluorotoluene, 4-fluorotoluene and 2-chlorotoluene.

Results from the present study show that, for the methyl substituted benzenes, there is a marked and almost linear increase in reactivity towards chlorine atoms with increasing number of methyl groups attached to the aromatic ring, Figure 2.14. An increase in reactivity with increasing degree of methyl substitution has also been observed in the reactions of these compounds with hydroxyl radicals [140] where the dominant reaction channel is addition to the ring and nitrate radicals [141] where the dominant reaction channel is abstraction from the alkyl substituent(s).

Figure 2.15 shows a linear free energy plot for reaction of chlorine atoms and hydroxyl radicals with a series of aromatic hydrocarbons. The general form of these correlations is a linear relationship between the logarithms of the rate constants for the reactions of Cl and OH with the aromatic substrates:

$$\log k_{Cl} = m \log k_{OH} + c$$

The basis for these empirical correlations comes from the thermodynamic expression of transistion-state theory, according to which a rate constant can be expressed in terms of the free energy of activation, ΔG^{ϕ}:

$$k = (\mathbf{k}T/h) \exp(-\Delta G^{\phi}/RT)$$

where **k** is the Boltzmann constant and h is Planck's constant. From the combination of these two equations a linear free energy relationship is obtained. This allows comparisons of reactivities permitting recognition of patterns of chemical behaviour and observation of deviations from such patterns.

Figure 2.15 shows no degree of linearity suggesting that the reaction mechanism for chlorine atoms with this series of aromatic compounds is different to that for reaction of hydroxyl radicals. Figure 2.16 shows a linear free energy plot of the rate constant data for reactions of chlorine atoms and nitrate radicals with aromatic hydrocarbons. This plot shows a reasonable degree of linearity, however, it should be noted that the same plot with the omission of ethylbenzene (Figure 2.17) shows a greater degree of linearity. It would appear from Figures 2.16 and 2.17 that the reported upper limit of the rate constant for reaction of nitrate radicals with ethylbenzene k ($NO_3 + C_6H_5C_2H_5$) = 6 x 10^{-16} cm^3 $molecule^{-1}$ s^{-1} [142], is in error and the true value is closer to 2 x 10^{-16} cm^3 $molecule^{-1}$ s^{-1}. The good linear free energy relationship observed between chlorine atoms and nitrate radicals strongly supports the abstraction channel for reaction of chlorine atoms with aromatic compounds.

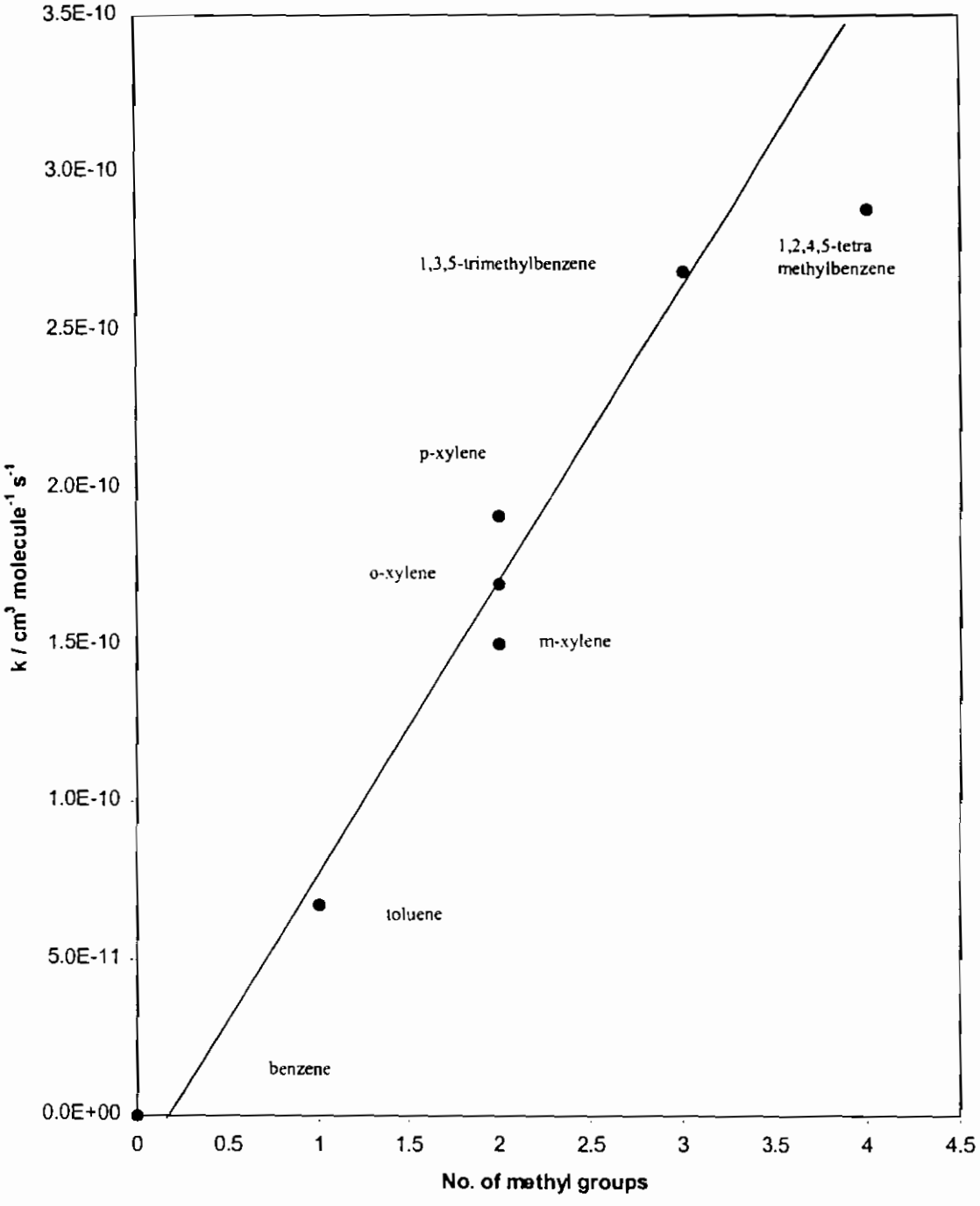

Figure 2.14. Rate constants for reaction of methyl-substituted benzenes with chlorine atoms versus number of methyl groups attached to the benzene ring

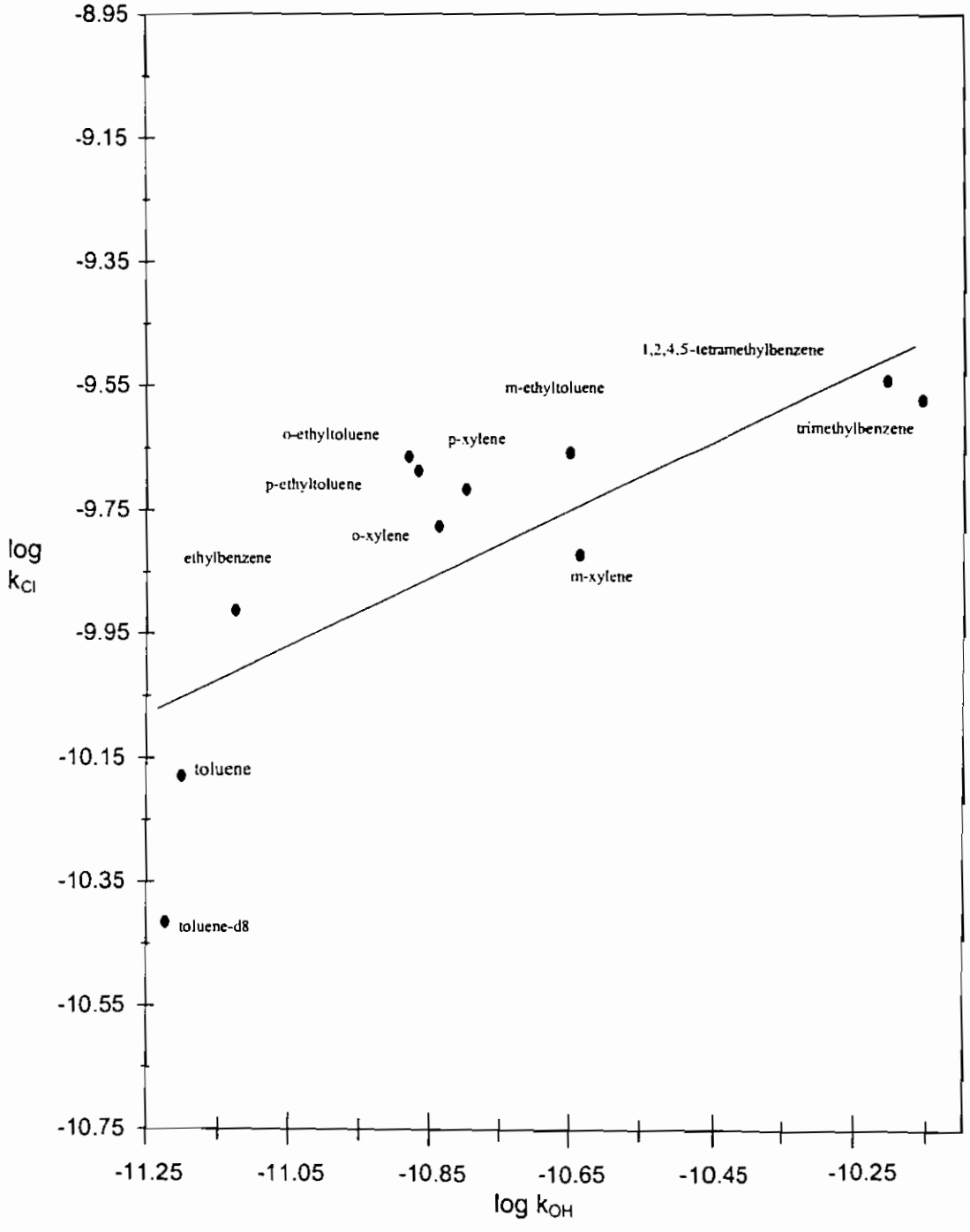

Figure 2.15. Linear free energy plot of the rate constants for the reactions of chlorine atoms and hydroxyl radicals with a series of aromatic hydrocarbons

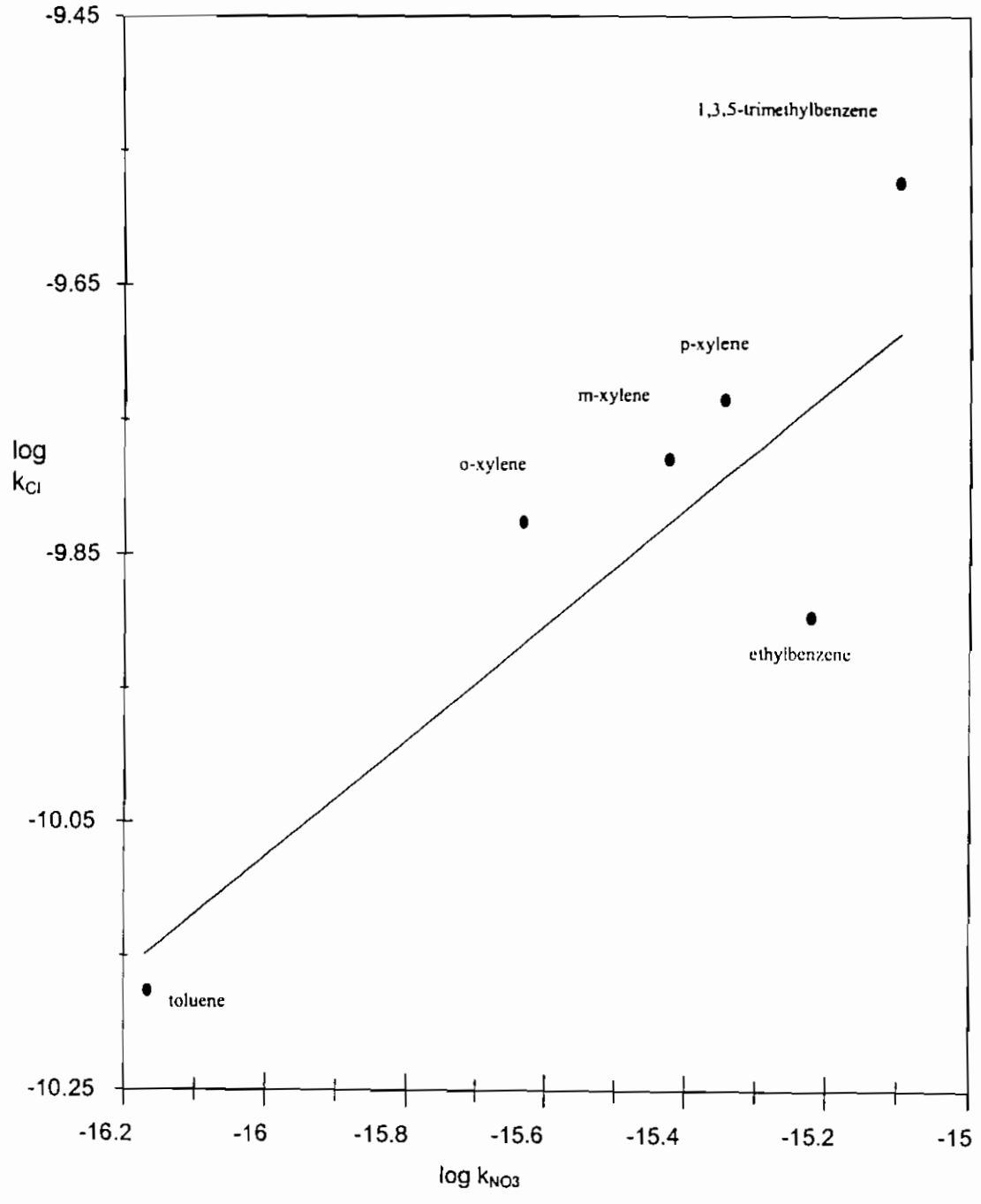

Figure 2.16. Linear free energy plot of the rate constants for the reactions of chlorine atoms and nitrate radicals with a series of aromatic hydrocarbons

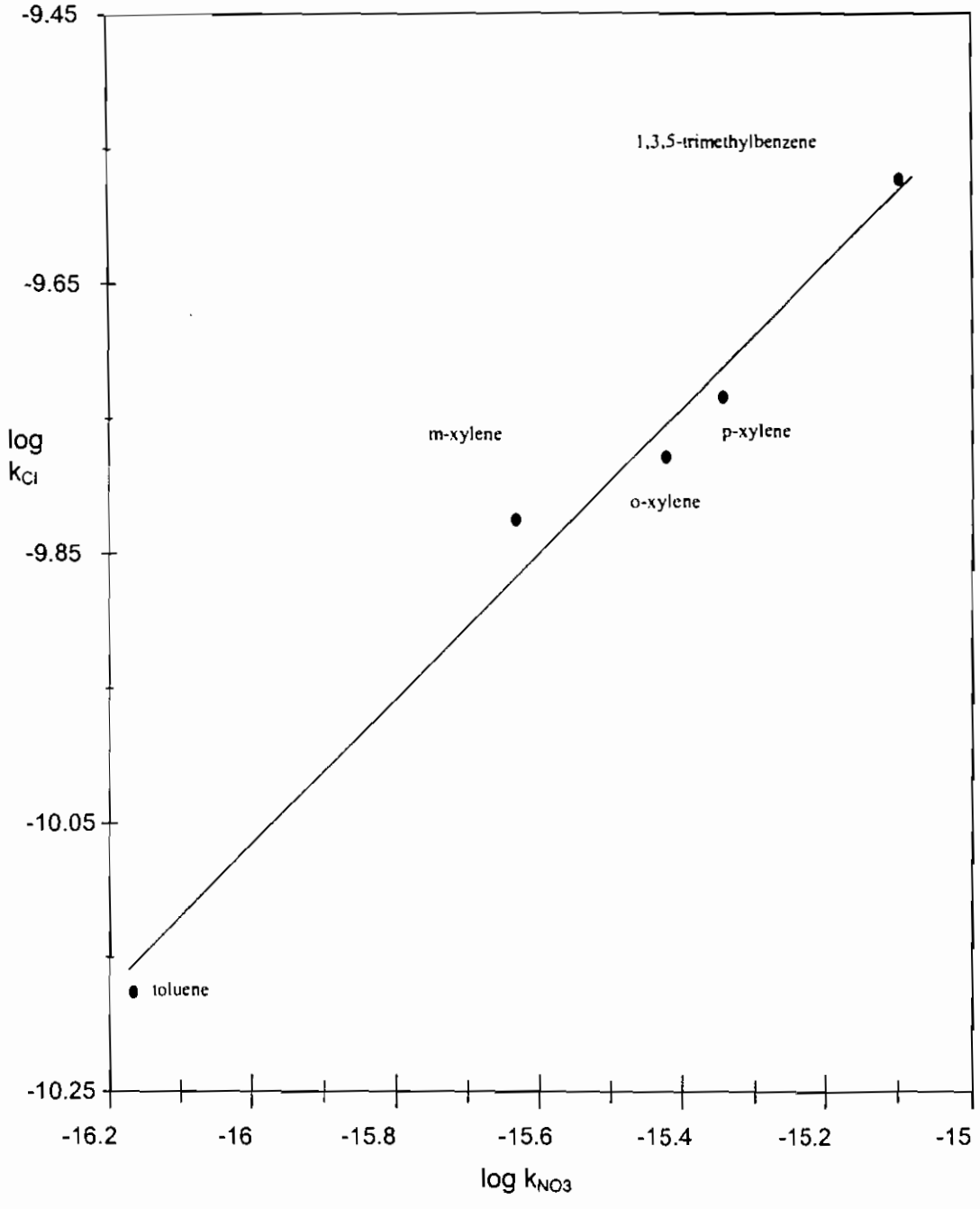

Figure 2.17. Linear free energy plot of the rate constants for the reactions of chlorine atoms and nitrate radicals with the same series of aromatic hydrocarbons as in Figure 2.16 with ethylbenzene omitted.

Wallington et al. [93] measured the rate constants for reaction of chlorine atoms with benzene, toluene, *o*-xylene, *m*-xylene and *p*-xylene in air at 298K and 1 atm. total pressure using a relative rate method. The investigators found toluene to be at least fourteen times more reactive than benzene. The rate constants for reaction of chlorine atoms with *o*-, *m*- and *p*-xylene were shown to be virtually indistinguishable and twice that of toluene. From these results the authors concluded that reaction of the methyl substituted aromatics with chlorine atoms proceeds by a mechanism involving H-atom abstraction from the methyl group(s).

Market and Pagsberg [101] studied the reaction of chlorine atoms with toluene using the absolute technique of pulse radiolysis combined with time-resolved ultraviolet spectroscopy. They found that the absorption spectrum of the transient species in the reaction corresponded to that of benzyl radicals ($C_6H_5CH_2$) and that there was no indication of transient absorption signals which could be assigned to an adduct. The authors concluded, in agreement with Wallington et al. [95], that the reaction of chlorine atoms with toluene proceeds exclusively via abstraction of a hydrogen atom from the methyl group.

Nozière et al. [98] investigated the reaction of chlorine atoms with toluene in 700 Torr of nitrogen diluent using a relative rate technique combined with Fourier transform infrared spectroscopy analysis of the reaction products. The major reaction products observed were benzyl chloride and benzyl dichloride with trace amounts of

benzaldehyde. The formation of benzyl chloride and benzyl dichloride can be rationalised in terms of the following mechanism:

$$C_6H_5CH_3 + Cl \rightarrow C_6H_5CH_2 + HCl \quad (2.29)$$

$$C_6H_5CH_2 + Cl_2 \rightarrow C_6H_5CH_2Cl + Cl \quad (2.30)$$

$$C_6H_5CH_2Cl + Cl \rightarrow C_6H_5CHCl + HCl \quad (2.31)$$

$$C_6H_5CHCl + Cl_2 \rightarrow C_6H_5CHCl_2 + Cl \quad (2.32)$$

The authors suggested that the formation of benzaldehyde was due to traces of molecular oxygen in the nitrogen diluent:

$$C_6H_5CH_2 + O_2 \rightarrow C_6H_5CH_2O_2 \quad (2.33)$$

$$2\ C_6H_5CH_2O_2 \rightarrow 2\ C_6H_5CH_2O + O_2 \quad (2.34)$$

$$2\ C_6H_5CH_2O_2 \rightarrow C_6H_5CH_2OH + C_6H_5CHO \quad (2.35)$$

$$C_6H_5CH_2O + O_2 \rightarrow C_6H_5CHO + HO_2 \quad (2.36)$$

Within the experimental uncertainties, the authors found that benzyl chloride, benzyl dichloride and benzaldehyde accounted for all of the observed loss of toluene. Hence the reaction of chlorine atoms with toluene gave 100% yield of benzyl radicals proving that the reaction proceeds exclusively by H-atom abstraction from the methyl group.

Kinetic data from this study shows that there is an increase in reactivity towards chlorine atoms with increasing length of the alkyl side chain. The rate constants obtained for toluene, ethylbenzene, n-propylbenzene and n-butylbenzene allow calculation of an average -CH_2- group rate constant for reaction with chlorine atoms of about 6 x 10^{-11} cm^3 $molecule^{-1}$ s^{-1}. This value is similar to the group rate constant estimated by Atkinson and Aschmann [89] for hydrogen atom abstraction by chlorine atoms from -CH_2- groups in alkanes (k_{-CH2-} = 5.6 x 10^{-11} cm^3 $molecule^{-1}$ s^{-1}). In a similar manner, the ethyltoluenes are more reactive towards chlorine atoms than the corresponding xylene isomers ($\Delta k_{Cl} \approx 6 \times 10^{-11}$ cm^3 $molecule^{-1}$ s^{-1} where Δk_{Cl} is the difference between $k_{average}(Cl + C_6H_4(CH_3)_2)$ and $k_{average}(Cl + C_2H_5C_6H_4CH_3)$). These differences in reactivity support the importance of the abstraction channel.

Additional evidence obtained in this study in support of hydrogen atom abstraction from the alkyl side chain comes from the existence of a significant kinetic isotope effect between toluene and toluene-d_8 (k_H/k_D = 1.79), *p*-xylene and *p*-xylene-d_6 (k_H/k_D = 1.9) and *p*-xylene and *p*-xylene-d_{10} (k_H/k_D = 1.9) and a smaller kinetic isotope effect between *o*-xylene and *o*-xylene-d_{10} (k_H/k_D = 1.23).

The primary deuterium isotope effect is due to the difference in the zero-point energy of the C-D and C-H bonds. The lower zero-point energy of the C-D bond leads to a loss of zero-point stretching vibration energy in the transition state compared to the C-H bond. The zero-point energy difference is about 5 kJ mol^{-1} which would give a value for k_H/k_D

of about 7. This magnitude varies and depends on the amount of bond forming and bond breaking or the symmetry of the transition state. Primary kinetic isotope effects of 2-8 are generally encountered though larger values occur when quantum mechanical tunnelling is involved. Secondary isotope effects are caused by differences in steric or hyperconjugative factors between the two isotopes. They are usually smaller in magnitude with $k_H/k_D \approx 1.5$.

The deuterium isotope effects measured in this study of k_H/k_D = 1.23 - 1.9 are low for primary isotope effects suggesting that the degree of bond breaking in the transition state is small. There is virtually no difference in the rate constants for reaction of chlorine atoms with *p*-xylene-d_{10} and *p*-xylene-d_6 indicating that the ring hydrogens are not involved in the abstraction process.

All the above findings support the conclusions of Wallington et al. [95], Markert and Pagsberg [101] and Nozière et al. [98] that the dominant, if not exclusive, reaction pathway for the gas phase chlorination of aromatic compounds is hydrogen atom abstraction from the alkyl substituent(s).

It is interesting to note that the presence of a halogen atom on the aromatic ring leads to a decrease in reactivity towards chlorine atoms with 2-fluorotoluene, k(Cl + 2-$C_6H_4CH_3F$) = 3.38 x 10^{-11} cm^3 $molecule^{-1}$ s^{-1}, being more unreactive than 2-chlorotoluene, k(Cl + 2-$C_6H_4CH_3Cl$) = 4.94 x 10^{-11} cm^3 $molecule^{-1}$ s^{-1}. This suggests that

the rate of hydrogen atom abstraction from an alkyl group by chlorine atoms is influenced by the presence of other substituents on the benzene ring. Halogen substituents withdraw electron density from the aromatic ring, with fluorine being more deactivating than chlorine. This leads to a reduction in reactivity toward the electrophilic chlorine atom. Conversely, alkyl substituents donate electron density to the benzene ring and hence an increase in the reactivity towards chlorine atoms is expected. This may explain why the xylenes, $k_{average}$ ($Cl + C_6H_4(CH_3)_2$) = 17 x 10^{-11} cm^3 $molecule^{-1}$ s^{-1}, are slightly more than twice and 1,3,5-trimethylbenzene, k($Cl + C_6H_3(CH_3)_3$) = 26.8 ± 1.8 x 10^{-11} cm^3 $molecule^{-1}$ s^{-1}, more than three times as reactive towards chlorine atoms as toluene, k($Cl + C_6H_5CH_3$) = 6.70 ± 0.41 x 10^{-11} cm^3 $molecule^{-1}$ s^{-1}. The rate constant obtained for reaction of chlorine atoms with 1,2,4,5-tetramethylbenzene, k($Cl + C_6H_2(CH_3)_4$) = 28.8 ± 1.5 x 10^{-11} cm^3 $molecule^{-1}$ s^{-1}, is somewhat lower than expected based on the above argument and may be due to steric hindrance.

The room temperature rate constants reported [141] for reaction of nitrate radicals with *o*-xylene, k($Cl + o\text{-}C_6H_4(CH_3)_2$ = 3.77 x 10^{-16} cm^3 $molecule^{-1}$ s^{-1}, *m*-xylene, k($Cl + m\text{-}C_6H_4(CH_3)_2$ = 2.33 x 10^{-16} cm^3 $molecule^{-1}$ s^{-1}, and *p*-xylene, k($Cl + p\text{-}C_6H_4(CH_3)_2$ = 4.53 x 10^{-16} cm^3 $molecule^{-1}$ s^{-1}, indicate that the order of reactivity is *para* > *ortho* > *meta*. The results from this study suggest that the order of reactivity towards chlorine atoms for the xylene isomers is also *para* > *ortho* > *meta*. Differences in reactivity between the

isomers can be explained via the resonance structures for the radicals obtained after hydrogen atom abstraction from the methyl group :

o-xylene radical

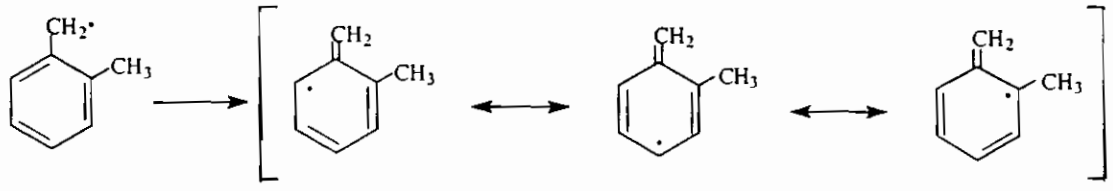

m-xylene radical

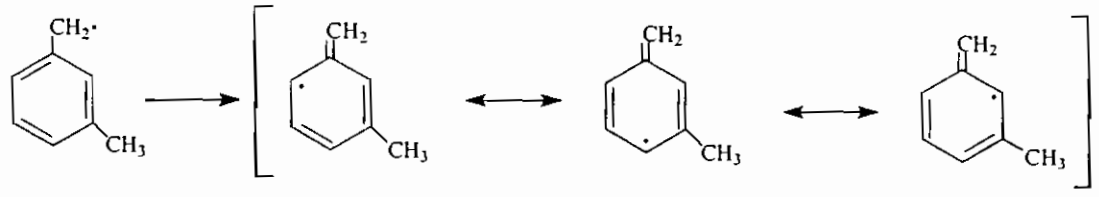

p-xylene radical

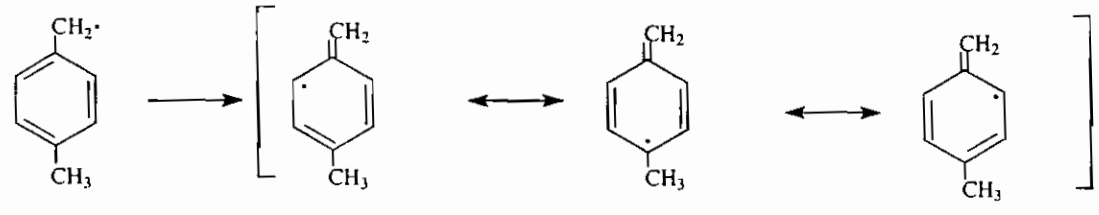

The radical resulting from the hydrogen atom abstraction from *o*- and *p*-xylene is stabilised by hyperconjugation between the lone electron and the methyl group. None

of the resonance structures for the *m*-xylene radical place the lone electron on the carbon attached to the methyl group therefore hyperconjugation cannot take place.

The ethyltoluenes might be expected to show the same the order of reactivity towards chlorine atoms as the corresponding xylene isomers but this is not observed. This is probably because the reactivity towards chlorine atoms ($\sim 2 \times 10^{-10}$ cm^3 molecule^{-1} s^{-1}) is close to the collision number and hyperconjugation effects are insignificant.

Atmospheric Implications

Table 2.6. shows the room temperature rate constants and atmospheric lifetimes (τ) for the aromatic compounds studied in this work with respect to reaction with chlorine atoms, hydroxyl and nitrate radicals.

$$\tau = 1 / k_X[X]$$

where [X] is the tropospheric concentration of chlorine atoms, hydroxyl radicals or nitrate radicals, and

k_X is the room temperature rate constant for the reaction of the substrate with chlorine atoms, hydroxyl radicals or nitrate radicals

Rate constants for reaction of aromatic hydrocarbons with chlorine atoms are between one and two orders of magnitude greater than with hydroxyl radicals. The concentration of OH radicals in the troposphere is approximately 1 x 10^6 cm^{-3} hence, should the concentration of chlorine atoms be in the range 10^3-10^5 cm^{-3} atmospheric loss by reaction with chlorine atoms will be significant. The data shown in Table 2.6 clearly shows that the atmospheric lifetimes with respect to reaction with chlorine atoms for all the aromatics, with the exception of benzene, are of the same order as the atmospheric lifetimes with respect to reaction with hydroxyl radicals (1-4 days). The atmospheric lifetimes due to reaction with nitrate radicals are much longer. These lifetime calculations clearly demonstrate that, with the exception of benzene, reaction with chlorine atoms could be a significant loss process for aromatic compounds in the atmosphere should the chlorine atom concentration be in the middle of the very poorly

constrained range of 10^3-10^6 cm^{-3}. The chlorine atom concentration is highest in coastal regions therefore loss of aromatic compounds via reaction with chlorine atoms may be significant in major urban areas located in coastal zones.

Table 2.6. Atmospheric lifetimes of a series of aromatic compounds with respect to reaction with chlorine atoms, hydroxyl radicals and nitrate radicals

Aromatic	[a] $10^{11} \times k_{Cl}$ cm^3 molecule^{-1}s^{-1}	[b] τ_{Cl} / days	$10^{12} \times k_{OH}$ cm^3 molecule^{-1}s^{-1}	[c] τ_{OH} / days	$10^{17} \times k_{NO3}$ cm^3 molecule^{-1}s^{-1}	[d] τ_{NO3} / months
benzene	<0.1	231.5	1.23 ± 0.37 [139]	18.8	< 3 [141]	50.7
toluene	6.70 ± 0.41	3.5	5.96 ± 1.49 [139]	3.9	6.8 ± 3.4 [141]	22.4
o-xylene	16.9 ± 0.8	1.4	13.7 ± 3.4 [139]	1.7	37.7 ± 5.3 [141]	4.0
m-xylene	15.0 ± 0.8	1.5	23.6 ± 5.9 [139]	1.0	23.3 ± 1.2 [141]	6.5
p-xylene	19.1 ± 0.6	1.2	14.3 ± 5.7 [139]	1.6	45.3 ± 3.2 [141]	3.4
1,3,5-trimethylbenzene	26.8 ± 1.6	0.9	57.4 ± 9.2 [139]	0.4	80.0 ± 6.4 [141]	1.9
1,2,4,5-tetramethylbenzene	28.8 ± 1.5	0.8	e		e	
o-ethyltoluene	21.9 ± 1.0	1.1	12.3 ± 4.9 [139]	1.9	e	
m-ethyltoluene	22.1 ± 1.1	1.0	19.2 ± 7.7 [139]	1.2	e	
p-ethyltoluene	20.7 ± 0.8	1.1	12.1 ± 4.8 [139]	1.9	e	
ethylbenzene	12.3 ± 0.3	1.9	7.1 ± 2.5 [139]	3.3	< 6 [141]	2.7
n-propylbenzene	21.9 ± 0.6	1.1	6.0 ± 1.8 [139]	3.9	e	
n-butylbenzene	28.0 ± 1.8	0.8	e		e	

Table 2.6 contd...

2-fluorotoluene	3.38 ± 0.4	6.8	e		e	
3-fluorotoluene	3.34 ± 0.3	6.9	e		e	
4-fluorotoluene	4.96 ± 0.5	4.7	e		e	
2-chlorotoluene	4.94 ± 0.8	4.7	e		e	

a this work

b [Cl] = 5×10^4 per cm^3; mid value of estimated range (10^3-10^6) [143]

c [OH] = 5×10^5 per cm^3; typical for remote continental location [144]

d [NO_3] = 2.5×10^8 per cm^3; typical for remote continental location [12]

e no kinetic data available

3 REFERENCES

1. S. Chapman, Q. J. R. Meteorol. Soc., **3**, 103, (1930).

2. B.J. Finlayson-Pitts and J.N. Pitts Jnr., "Atmospheric Chemistry: Fundamentals and Experimental Techniques", J. Wiley & Sons (1986).

3. M.J. Molina and F.S. Rowland, Nature, **249**, 810, (1974).

4. J. Farman, B. Gardiner and J. Shanklin, Nature, **315**, 207, (1985).

5. D.J. Hoffmann, S.J. Oltmans, J.M. Harris, B.J. Johnson & J.A. Lathrop, J. Geophys. Res.-Atm., **102**, 8931, (1997).

6. Y.B. Jiang, Y.L. Yung & R.W. Zurek, J. Geophys. Res.-Atm., **101**, 8985, (1996).

7. G.L. Manney, R.W. Zurek, L. Froidevaux & J.W. Waters, Geophys. Res. Lett., **22**, 2941, (1995).

8. G.L. Manney, M.L. Santee, L. Froidevaux, J.W. Waters & R.W. Zuerek, Geophys. Res. Lett., **23**, 3203, (1996).

9. D.P. Donovan, J.C. Bird, J.A. Whiteway, T.J. Duck, S.R. Pal, A.I. Carswell, J.W. Sandilands & J.W. Kaminski, Geophys. Res. Lett., **23**, 3317, (1996).

10. R.M. Harrison, in "Pollution: Causes, Effects, and Control", 2nd ed., ed. R.M. Harrison, The Royal Society of Chemistry, (1990).

11. R. Atkinson, J. Phys. Chem. Ref. Data, Monograph 2, 1, (1994).

12. R.P. Wayne, I. Barnes, P. Biggs, J.P. Burrows, C.E. Canosa-Mas, J. Hjorth, G. LeBras, G.K. Moortgat, D. Perner, G. Poulet, G. Restelli, and H. Sidebottom, Atmos. Environ., **25A**, 1, (1991).

13. S.E. Manahan, "Environmental Chemistry", 6th ed., Lewis Publishers, (1994).

14. C.D. O'Dowd, M.H. Smith, I.E. Consterdine & J.A. Lowe, Atmos. Environ., **31**, 73, (1997).

15. R.J. Cicerone, Rev. Geophys. Space Phys., **19**, 123, (1981).

16. W.C. Keene, A.A.P. Pszenny, D.J. Jacob, R.A. Duce, J.N. Galloway, J.J. Schultz-Tokos Jr., H. Sievering, and J.F. Boatman, Global Biogeochem. Cycles, **4**, 407, (1990).

17. H. Cauer, Der Balneologie, **8**, 345, (1941).

18. H. Egnér & E. Eriksson, Tellus, **7**, 135, (1955).

19. C.-G. Rossby & H. Egnér, Tellus, **7**, 118, (1955).

20. H. Cauer, in "Compendium of Meterology", Am. Met. Soc., Boston, pp.1126, (1951).

21. B.C.V. Oddie, Roy. Met. Soc. Quart. J., **85**, 163, (1959).

22. R.C. Robbins, R.D. Cadle & D.L. Eckhardt, J. Met., **16**, 53, (1959).

23. C.E. Junge, Tellus, **9**, 528, (1957).

24. P. Beichert & B.J. Finlayson-Pitts, J. Phys. Chem., **100**, 15218, (1996).

25. T.E. Graedel & W.C. Keene, Pure & Appl. Chem., **68**, 1689, (1996).

26. B.J. Finlayson-Pitts, M.J. Ezell and J.N. Pitts Jr., Nature, **337**, 241, (1989).

27. J.K.S. Wan, J.N. Pitts Jr., P. Beichert & B.J. Finlayson-Pitts, Atmos. Environ., **30,** 3109, (1996).

28. S. Langer, R.S. Pemberton & B.J. Finlayson-Pitts, J. Phys. Chem. A., **101**, 1277, (1997).

29. R. Vogt & B.J. Finlayson-Pitts, J. Phys. Chem., **98**, 3747, (1994).

30. C. Zetzsch & W. Behnke, Ber. Bunsenges. Phys. Chem., **96**, 3, (1992).

31. W.H. Schroeder & P. Urone, Environ. Sci. Technol., **8**, 756, (1974).

32. B.J. Finlayson-Pitts, Nature, **306**, 676, (1983).

33. W. Behnke, C. George, V. Scheer & C. Zetzsch, J. Geophys. Res., **102**, 3798, (1997).

34. H.C. Allen, J.M. Laux, R. Vogt, B.J. Finlayson-Pitts & J.C. Hemminger, J. Phys. Chem., **100**, 6371, (1996).

35. J.M. Laux, T.F. Fister, B.J. Finlayson-Pitts & J.C. Hemminger, J. Phys. Chem., **100**, 19891, (1996).

36. W. Behnke & C. Zetzsch, in "Ozone in the Atmosphere, Proceedings of the Quadrennial Ozone Symposium 1988 and Tropospheric Ozone Workshop", edited by B.D. Bojkov & P. Fabian, pp. 519, A. Deepak, Hampton, Va., (1989).

37. T.G. Koch, S.F. Banham, J.R. Sodeau, A.B. Horn, M.R.S. McCoustra & M.A. Chesters, J. Geophys. Res., **102**, 1513, (1997).

38. H.B. Singh and J.F. Kasting, J. Atmos. Chem., **7**, 261, (1988).

39. W.B. DeMore, J.J. Margitan, M.J. Molina, R.T. Watson, D.M. Golden, R.F. Hampson, M.J. Kurylo, C.J. Howard & A.R. Ravishankara, "Chemical Kinetics and Photochemical Data for Use in Stratospheric Modeling, Eval. No. 7, JPL Publication 85-37, (1985).

40. WMO, Atmospheric Ozone, Halogenated Species - Chapter 11, WMO report no. 16, pp. 605, (1985).

41. A. Pszenny, W. Keene, D. Jacob, S. Fan, J. Maben, M.P. Zetwo, M. Springer-Young and J. Galloway, Geophys. Res. Lett., **20**, 699, (1993).

42. B.T. Jobson, H. Niki, Y. Yokouchi, J. Bottenheim, F. Hopper, and R. Leatich, J.Geophys. Res., **99**, 25355, (1994).

43. H.B. Singh, G.L. Gregory, B. Anderson, E. Browell, G.W. Sachse, D.D. Davis, J. Crawford, J.D. Bradshaw, R. Talbot, D.R. Blake, D. Thornton, R. Newell and J. Merrill, J. Geophys. Res., **101**, 1907, (1996).

44. J. Rudolph, R. Koppman & CH. Plass-Dülmer, Atmos. Environ., **10/11**, 1887-1894, (1996).

45. H.B. Singh, A.N. Thakur, Y.E. Chen & M. Kanakidou, Geophys. Res. Lett., **23**, 1529, (1996).

46. G.A. Impey, P.B. Shepson, D.R. Hastie, L.A. Barrie & K.G. Anlauf, J. Geophys. Res., **102**, 16,005, (1997).

47. O.W. Wingenter, M.K. Kubo, N.J. Blake, T.W. Smith Jr., D.R. Blake & F.S. Rowland, J. Geophys. Res., **101**, 4331, (1996).

48. C.W. Spicer, E.G. Chapman, B.J. Finlayson-Pitts, R.A. Plastridge, J.M. Hubbe, J.D. Fast and C.M. Berkowitz, Nature, **394**, 353, (1998).

49. P.B. Shepson, A.-P. Sirju, J.F. Hopper, L.A. Barrie, V. Young, H. Niki & H. Dryfhout, **101**, 21081, (1996).

50. A. Wegner, G.P. Stiller, T. von Clarmann, O. Trieschmann & H. Fischer, Geophys. Res. Lett., **24**, 849, (1997).

51. G.E. Shaw, J. Geophys. Res., **96**, 22369, (1991).

52. D.H. Lowenthal, R.D. Borys, C.F. Rogers, J.C. Chow, R.K. Stevens, J.P. Pinton & J.M. Ondov, Geophys. Res. Lett., **20**, 691, (1993).

53. R.Stevens, J. Pinto, Y. Mamane, J. Ondov, M. Abdulraheem, N. Al-Majed, M. Sadek, W. Cofer, W. Ellenson & R. Kellog, Wat. Sci. Tech., **27**, 223, (1993).

54. P.J. Sheridan, R.C. Schnell, D.J. Hoffman, J.M. Harris & T. Deshler, Geophys. Res. Lett., **19**, 389, (1992).

55. O. Hov, Atmos. Environ., **19**, 471, (1985).

56. F. Stuhl & H. Niki, J. Chem. Phys., **57**, 3671, (1972).

57. R.K. Lengel & D. Crossley, J. Chem. Phys., **67**, 2085, (1977).

58. I.T.N. Jones & K.D. Bayes, Chem. Phys. Lett., **11**, 163, (1971).

59. R.G.W. Norrish & G. Porter, Nature, **164**, 658, (1949).

60. N.R. Greiner, J. Chem. Phys., **46**, 2795, (1967).

61. W.J. Marinelli & H.S. Johnson, J. Chem. Phys., **77**, 1225, (1982).

62. J.J. Margitan & R.T. Watson, J. Phys. Chem., **86**, 3819, (1982).

63. P.H. Wine, N.M. Kreutter & A.R. Ravishankara, J. Phys. Chem., **83**, 3191, (1979).

64. C. Morley & I.W.M. Smith, J. Chem. Soc. Faraday Trans. 2, **68**, 1016, (1972).

65. D.D. Davis, W. Braun, and A.M. Bass, Int. J. Chem. Kinet., **2**, 101, (1970).

66. P. Beichert, L. Wingen, J. Lee, R. Vogt, M.J. Ezell, M. Ragains, R. Neavyn & B.J. Finlayson-Pitts, J. Phys. Chem., **99**, 13156, (1995).

67. G. Poulet, G. LeBras and J. Combourieu, J. Chimie Physique, **71**, 101, (1974).

68. M.A.A. Clyne and R.F. Walker, J. Chem. Soc. Faraday Trans.I, **69**, 1547, (1973).

69. M.T. Leu and W.B. DeMore, Chem. Phys. Lett., **41**, 121, (1976).

70. R.T. Watson, G. Machado, S. Fischer and D.D. Davis, J. Chem. Phys., **65**, 2126, (1976).

71. D.A. Whytock, J.H. Lee, J.V. Michael, W.A. Payne and L.J. Stief, J. Chem. Phys., **66**, 2690, (1977).

72. J.V. Michael and J.H. Lee, Chem. Phys. Lett., **51**, 303, (1977).

73. R.G. Manning and J.J. Kurylo, J. Phys. Chem., **81**, 291, (1977).

74. M.S. Zahniser, B.M. Berquist and F. Kaufman., Int. J. Chem. Kinet., **10**, 15, (1978).

75. G. Poulet, G. LeBras, and J. Combourieu, Paper presented at the WMO meeting in Toronto, WMO #511, 289, (1978).

76. L. Keyser, J. Chem. Phys., **69**, 214, (1978).

77. C.L. Lin, M.T. Leu and W.B. DeMore, J. Phys. Chem., **82**, 1772, (1978).

78. H.O. Pritchard, J.B. Pyke and A.F. Trotman-Dickenson, J. Am. Chem. Soc., **76**, 1201, (1954).

79. J.H. Knox, and R.L. Nelson, Trans. Faraday Soc., **55**, 937, (1959).

80. J.H. Knox, Chemistry and Industry, 1631, (1955).

81. H.O. Pritchard, J.B. Pyke and A.F. Trotman-Dickenson, J. Am. Chem. Soc., **77**, 2629, (1955).

82. F.S. Lee and F.S. Rowland, J. Phys. Chem., **81**, 86, (1977).

83. H. Niki, P.D. Maker, C.M. Savage and L.P. Breitenbach, Int. J. Chem. Kinet., **12**, 1001, (1980).

84. P.H. Taylor, Z. Zhiang and B. Dellinger, Int. J. Chem. Kinet., **25**, 9, (1993).

85. P.H. Wine and D.H. Semmes, J. Phys. Chem., **87**, 3572, (1983).

86. R.S. Lewis, S.P. Sander, S.Wagner and R.T. Watson, J. Phys. Chem., **84**, 2009, (1980).

87. G.S. Tyndall, J.J. Orlando, T.J. Wallington, M. Dill and E.W. Kaiser, Int. J. Chem. Kinet., **29**, 43, (1997).

88. R. Atkinson and S.M. Aschmann, Int. J. Chem. Kinet., **17**, 33, (1985).

89. R. Atkinson and S.M. Aschmann, Int. J. Chem. Kinet., **19**, 1097, (1987).

90. T.J. Wallington, L.M. Skewes, W.O. Siegl, C-H Wu and S.M. Japar, Int. J. Chem. Kinet., **20**, 867, (1988).

91. S.M. Aschmann and R.Atkinson, Int. J. Chem. Kinet., **27**, 613, (1995).

92. T.J. Wallington, L.M. Skewes and W.O.Siegl, , J. Phys. Chem., **93**, 3649, (1989).

93. K. Kambanis, Y.G. Lazarou and and P. Papagiannakopoulos, Int. J. Chem. Kinet., **27**, 343, (1995).

94. M.L. Ragains & B.J. Finlayson-Pitts, J. Phys. Chem. A, **101**, 1509, (1997).

95. T.J. Wallington, L.M. Skewes and W.O. Siegl, J. Photochem. Photobiol. A: Chem., **45**, 167, (1988).

96. E.W. Kaiser and T.J. Wallington, J. Phys. Chem., **100**, 9788, (1996).

97. A. Bierbach, I. Barnes and K.H. Becker, Int. J. Chem. Kinet., **28**, 565, (1996).

98. B. Nozière, R. Lesclaux, M.D. Hurley, M.A. Dearth and T.J. Wallington, J. Phys. Chem., **98**, 2864, (1994).

99. F. Berho, M-T. Rayez and R. Lesclaux, poster presented at 14th International Symposium on Gas Kinetics, Leeds, U.K. (1996).

100. J.C. Shi & M.J. Bernhard, Int. J. Chem. Kinet., **29**, 349, (1997).

101. F. Markert and P. Pagsberg, Chem. Phys. Lett., **209**, 445, (1993).

102. J-Y. Park, I.R. Slagle and D. Gutman, J.Phys. Chem., **87**, 1812, (1983).

103. J.J. Orlando, G.S. Tyndall, T.J. Wallington & M. Dill, Int. J. Chem. Kinet., **28**, 433, (1996).

104. H. Niki, P.D. Maker, C.M. Savage and L.P. Breitenbach, J. Phys. Chem., **89**, 588, (1985).

105. T.J. Wallington, J.M. Andino, J.C. Ball and S.M. Japar, J. Atmos. Chem., **10**, 301, (1990).

106. E. Tschuikow-Roux, F. Faraji, S. Paddison, J. Niedzielski and K. Mizokawa, J. Phys. Chem., **92**, 1488, (1988).

107. E.C. Tuazon, R. Atkinson and S. B. Corchnoy, Int. J. Chem. Kinet., **24**, 639, (1992).

108. T.J. Wallington, J.C. Ball, O.J. Nielsen and E. Bartkiewicz, J. Phys. Chem., **96**, 1241, (1992).

109. E. Tschuikow-Roux, T. Yano and J. Niedzielski, J. Chem. Phys., **82**, 65, (1985).

110. J.P. Sawerysyn, A. Talhaoui, B. Meriaux and P. Devholder, Chem. Phys. Lett., **198**, 197, (1992).

111. S. Glavas and J. Heicklen, J. Photochem., **31**, 21, (1985).

112. T. Yano and E. Tschuikow-Roux, J. Photochem., **32**, 25, (1986).

113. T.J. Wallington and M.D. Hurley, Chem. Phys. Lett., **189**, 437, (1992).

114. R.F. Warren and A.R. Ravishankara, Int. J. Chem. Kinet., **25**, 833, (1993).

115. T.J. Wallington, M.M. Hinman, J.M. Andino, W.O. Siegl and S.M. Japar, Int. J. Chem. Kinet., **22**, 665, (1990).

116. G.S. Tyndall, J.J.Orlando, T.J.Wallington, J.Sehested and O.J.Nielsen,, J. Phys. Chem., **100**, 660, (1996).

117. O.J. Nielsen, H.W. Sidebottom, M. Donlon and J. Treacy, Chem. Phys. Lett., **178**, 163, (1991).

118. G. Poulet, G. Laverdet, J.L. Jourdain and G. Le Bras, J. Phys. Chem., 88, 6259, (1984).

119. M.J. Kurylo and G.L. Knable, J. Phys. Chem., **88**, 3305, (1984).

120. H. Niki, P.D. Maker, C.M. Savage and L.P. Breitenbach, Int. J. Chem. Kinet., **12**, 915, (1980).

121. S. Koch and G.K. Moortgat, Chem. Phys. Lett., **173**, 531, (1990).

122. T.J. Wallington, J.C. Ball, A.M. Straccia, M.D. Hurley, E.W. Kaiser, M. Dill, W.F. Schneider & M. Bilde, Int. J. Chem. Kinet., **28**, 627, (1996).

123. S. Langer, E. Ljungström, I. Wängberg, T.J. Wallington, M.D. Hurley & O.J. Nielsen, Int. J. Chem. Kinet., **28**, 299, (1996).

124. B.E.R. Olsson, M. Hallquist, E. Ljunström & J. Davidsson, Int. J. Chem. Kinet., **29**, 195, (1997).

125. G. Poulet, G. Laverdet and G. Le Bras, J. Phys. Chem., **85**, 1892, (1981).

126. D.J. Scollard, J.J. Treacy, H.W. Sidebottom, C. Balestra-Garcia, G. Laverdet, G. Le Bras, H. Mac Leod and S. Téton, J. Phys. Chem., **97**, 4683, (1993).

127. W.A. Payne, D.F. Nava, F.L. Nesbitt and L.J. Stief, J. Phys. Chem., **94**, 7190, (1990).

128. M. Bartels, K. Hoyermann and U. Lange, Ber. Bunsenges Phys. Chem., **93**, 423, (1989).

129. L. Nelson, O. Rattigan, R. Neavyn, H. Sidebottom, J. Treacy and O.J. Nielsen, Int. J. Chem. Kinet., **22**, 1111, (1990).

130. R. Atkinson, J. Phys. Chem. Ref. Data, 26, 215, (1997).

131. W.B. DeMore, S.P. Sander, C.J. Howard, A.R. Ravishankara, D.M. Golden, C.E. Kolb, R.F. Hampson, M.J. Kurylo, and M.J. Molina, "Chemical Kinetics and Photochemical Data for Use in Stratospheric Modeling, Eval. No. 12, JPL Publication 97-4, (1997).

132. V. Seeley, J.T. Jayne and M.J. Molina, J. Phys. Chem., **100**, 4019, (1996).

133. J. S. Pilgrim, A. McIlroy & C. A. Taatjes, J. Phys. Chem. A, **101**, 1873, (1997).

134. P.A. Hooshiyar and H. Niki, Int. J. Chem. Kinet., **27**, 1197, (1995).

135. M. Bartels, J. Edelbuttel-Einhaus & K. Hoyermann, 22nd Symposium (International) on Combustion / The Combustion Institute, 1041, (1988).

136. A. Notario, A. Mellouki & G. LeBras, private communication.

137. R. Atkinson, D.L. Bauch, R.A.Cox, R.F. Hampson, Jr., J.A. Kerr, M.J. Rossi and J. Troe, J. Phys. Chem. Ref. Data, **26**, 1329, (1997).

138. P.D. Lightfoot, R.A. Cox, J.N. Crowley, M. Destriau, G.D. Hayman, M.E. Jenkin, G.K. Moortgat and F. Zabel, Atmos. Environ., **26A**, 1805, (1992).

139. R. Atkinson, J. Phys. Chem. Ref. Data, Monograph 1, **1**, (1989).

140. R. Atkinson, Chem. Rev., **86**, 69, (1986).

141. R.J. Atkinson, J. Phys. Chem. Ref. Data, **20**, 459, (1991).

142. R. Atkinson, S.M. Aschmann and A.M. Winer, Env. Sci. Tech., **21**, 1123, (1987).

143. T.E. Graedel and W.C. Keene, Global Biogeochem. Cycles, **9**, 47, (1995).

144. M.J. Campbell, K. Sheppard and B.F. Au, Geophys. Res. Lett., **6**, 175, (1979).